

# Advection and diffusion in a three dimensional chaotic flow

X. Z. Tang\*

*Department of Applied Physics, Columbia University, New York, NY 10027*

A. H. Boozer

*Department of Applied Physics, Columbia University, New York, NY 10027  
and Max-Planck Institut für Plasmaphysik, Garching, Germany*

(June 25, 2018)

The advection-diffusion equation is studied via a global Lagrangian coordinate transformation. The metric tensor of the Lagrangian coordinates couples the dynamical system theory rigorously into the solution of this class of partial differential equations. If the flow has chaotic streamlines, the diffusion will dominate the solution at a critical time, which scales logarithmically with the diffusivity. The subsequent rapid diffusive relaxation is completed on the order of a few Lyapunov times, and it becomes more anisotropic the smaller the diffusivity. The local Lyapunov time of the flow is the inverse of the finite time Lyapunov exponent. A finite time Lyapunov exponent can be expressed in terms of two convergence functions which are responsible for the spatio-temporal complexity of both the advective and diffusive transports. This complexity gives a new class of diffusion barrier in the chaotic region and a fractal-like behavior in both space and time. In an integrable flow with shear, there also exist fast and slow diffusion. But unlike that in a chaotic flow, a large gradient of the scalar field across the KAM surfaces can be maintained since the fast diffusion in an integrable flow is strictly confined within the KAM surfaces.

PACS numbers: 47.10.+g, 52.30.-q, 05.45.+b

Keywords: Advection-diffusion equation, finite time Lyapunov exponent,  $\hat{s}$  line, diffusion barriers, hamiltonian chaos, fractal, mixing

## I. INTRODUCTION

### A. Motivation

The transport of a passive scalar  $\phi$  embedded in a fluid flow is governed by the advection-diffusion equation [1],

$$\partial\phi/\partial t + \mathbf{v} \cdot \nabla\phi = -(\nabla \cdot \Gamma_d)/\rho \quad (1)$$

with  $\mathbf{v}(\mathbf{x}, t)$  the fluid velocity,  $\rho$  the fluid density, and  $\Gamma_d = -\rho D \nabla\phi$  the diffusive flux. In its most primitive form,  $D$  is just the molecular diffusivity which is typically a small number, giving rise to an unphysically long characteristic diffusive time scale  $L^2/D$ . Being a linear equation, the non-triviality of the advection-diffusion equation comes from the flow velocity field  $\mathbf{v}(\mathbf{x}, t)$ . The purpose of this paper is to illustrate the general properties of the solution to the advection-diffusion equation in the case of a three dimensional chaotic flow. Our method [2] is based on a global Lagrangian coordinate transformation, which rigorously couples the dynamical system theory [3] into the solution of the advection-diffusion equation. The finite time Lyapunov exponent and the geometry of the so-called  $\hat{s}$  lines play the central roles in our theory [2], which is a distinct feature from other works in this area.

The standard treatment [4,5] of the advection-diffusion equation presumes a turbulent background flow, the so-called turbulent mixing problem. A method of averaging [e.g. [5]] is employed to separate the rapidly fluctuating component from the statistical mean. The effect of the fluctuating flow component is then modeled as an effective diffusivity [4] leading to enhanced mixing. This approach is justified by the wide separation of the correlation scales in the mean and the fluctuating flow velocity components [4–6].

Actually a smooth, non-turbulent, flow with chaotic fluid trajectories gives fundamentally different solutions to the advection-diffusion equation than a non-chaotic, or integrable, flow. The smoothness of the flow field precludes the method of averaging employed in the turbulent mixing theory. Existing literature on chaotic mixing largely concerns with the ideal advection equation [ $D = 0$  in equation (1)] whose solution is found by following the Lagrangian trajectories, for more details see section I B. The diffusive effect, i.e. right-hand-side of equation (1), is usually treated

---

\*Email: tang@chaos.ap.columbia.edu

as an add-on on the Lagrangian trajectory picture. For example, it has been modeled by a stochastic perturbation to the Lagrangian trajectories [*i.e.* a Langevin equation], or by a Gaussian smoothing kernel on the Lagrangian trajectories.

Most previous work [see section IB for detail] on chaotic mixing circumvents the advection-diffusion equation by working with the Lagrangian description of the fluid directly. This permits the utilization of dynamical system theory, particularly the multiplicative ergodic theorem [20] and the geometrical method, which leads to new insights unavailable in the usual Eulerian picture. A numerical solution of equation (1) using an Eulerian PDE solver has no obvious connection with the crucial features like KAM islands, chaotic components, or Lyapunov exponents. On the other hand, the efficiency and reliability of numerical PDE solvers for following the global solution for a long time requires an understanding of the properties of the solution and the features that define the range of validity of the numerical scheme. This is the primary motivation for our previous work in the two dimensional case and the current treatment for the three dimensional case.

The basic difference between our approach and those reviewed in section IB is that we directly solve the advection-diffusion equation including the effects of a finite diffusivity. The need to keep the diffusion term, despite the smallness of  $D$ , will become obvious once we obtain the full solution. The most obvious requirement for keeping a small  $D$  comes from the time for diffusion [the right-hand side of equation (1)] to dominate the solution, which has a logarithmic dependence on  $D$ . In a general context, the diffusion term is a singular perturbation to the pure advection equation. Mathematically it changes the characteristics, or type, of the underlying PDE. Physically it is responsible for removing the time reversibility of the physical process. This can be quantitatively explained by examining the mean variance of the passive scalar  $\phi$ ,

$$S \equiv - \int (\phi^2/2) d^3\mathbf{x}.$$

For a bounded system, it is straightforward to show that the entropy-like quantity  $S$  would increase or saturate only if  $D$  does not vanish, see equation (11).

In the next section we will briefly review some related work on chaotic mixing, ranging from chaotic advection, hamiltonian transport theory, to fractional kinetic theory. Neither the list of topics nor the literature cited can be exhaustive, but they give a reasonable perspective for contrasting our approach and results. For those familiar with the literature, section IB can be skipped in its entirety.

## B. A brief review of related work

As one of the primary physical applications of the chaos theory, it was recognized [7] in the eighties that smooth (laminar) flow could also lead to efficient mixing, as long as the flow trajectories are non-integrable or chaotic [for a sampling of experimental work, see [8,9]]. Despite the variants in name (chaotic advection or Lagrangian turbulence [7], hamiltonian transport theory [10], and fractional kinetic theory [11]), these treatments make the same assumption of ignoring the right-hand-side (diffusion) term in equation (1) and are, therefore, concerned with an ideal advection equation:

$$\partial\phi/\partial t + \mathbf{v}(\mathbf{x}, t) \cdot \nabla\phi = 0, \quad \text{or} \quad d\phi/dt = 0. \tag{2}$$

The mathematical solution to the advection equation is remarkably straightforward. Since the passive scalar is frozen into the fluid element, the distribution function  $\phi$  at arbitrary time is found by following the trajectory of each fluid element,

$$d\mathbf{x}(\xi, t)/dt = \mathbf{v}(\mathbf{x}, t), \tag{3}$$

with the initial condition  $\mathbf{x}(\xi, t = 0) = \xi$ . After integrating equation (3) to obtain  $\mathbf{x}(\xi, t)$  the solution to the ideal advection equation is  $\phi(\mathbf{x}(\xi, t), t) = \phi(\xi, t = 0)$ .

Reducing the solution of the advection equation to an integration of flow trajectories not only simplifies the problem, but also allows the theory of dynamical systems to be utilized for classifying the trajectories and the associated mixing properties [23]. The crudest estimate is entirely based on topology and the intuitive criteria that ergodicity implies good mixing. A plot of the Poincare section of the flow then becomes the standard tool. For example, on the Poincare section of a two-dimensional time-periodic flow, integrable trajectories lie on topological circles (so-called regular component, or KAM tori in hamiltonian mechanics) but non-integrable or chaotic trajectories fill a finite area (so-called irregular component). Integrable trajectories can divide the space into an infinite set of ergodic subregions. The integrable or regular, regions consist of closed lines or surfaces, so they are poor for mixing. Only chaotic regions,

*i.e.*, the irregular components, occupy a finite volume, which is required for good mixing. It is still an unresolved mathematical problem whether the irregular component occupies a finite measure. The difficulty lies in the fact that numerous regular components are embedded in an irregular component and the summation of those infinitely many small regular regions may not be small. However, this subtlety is not crucial for physical applications. If one goes back to the original advection-diffusion equation, any small but finite diffusivity would impose a cut-off for the smallest spatial scale on which one needs to worry about the regular islands. This effectively guarantees that a chaotic zone occupies finite volume for the purpose of passive scalar transport.

Although chaotic advection and hamiltonian transport theory in principle are entirely different subjects, they are often mathematically equivalent. An example is a divergence-free, two-dimensional time-periodic fluid flow, which is mathematically equivalent to a one and a half degree of freedom hamiltonian system. A major advance in understanding was the discovery of the cantorus [12], an invariant curve or surface similar to an KAM surface but with the crucial difference of its being on a cantor set. In other words, a cantorus is a KAM-like structure but with numerous holes so it can not separate an irregular component. The trajectories ‘leak’ through the cantori in a peculiarly orderly fashion, much like going through a revolving door, hence the name turnstile [13]. The cantori act as practical borders partitioning one ergodic irregular component into different subcomponents which have fast mixing within but much slower advective transport across. Motivated by this separation of time scales, a Markov tree model [14] was introduced to describe the slow mixing between the subcomponents separated by the cantori. Another less efficient but mathematically rigorous approach, the so-called lobe dynamics [15], generalized the idea of turnstiles for the advective transport across the boundary set by the invariant manifolds of any hyperbolic or normally hyperbolic sets. In effect, it calculates the advective flux by following the trajectories through a sequence of “revolving doors” (turnstile) on the otherwise closed boundaries. The boundaries are formed by the global invariant manifolds of hyperbolic sets, so they in principle could provide an arbitrarily fine partition of the space. In practice, the lobe dynamics become exponentially complicated as time proceeds so it is usually thought to be applicable for only a short time. The same argument also shows it is suitable for tracing initially isolated distribution but not for following the time evolution of a spatially-extended initial distribution. The reliance on the invariant manifolds also limits the application since their existence is not obvious for time quasi-periodic or aperiodic flows.

In the same spirit as using a diffusion equation to model Brownian motion [16], statistical approaches have also been advanced to model the chaotic advective transport as a diffusion process alone. The earliest work of this kind was due to Rechester and Rosenbluth [17] who modeled the chaotic motion of the electrons due to stochastic magnetic field lines in a toroidal magnetic confinement device by an effective diffusion coefficient. The Rechester-Rosenbluth diffusivity is unusual since it is based on a quasi-linear calculation [18] for the rate of average squared separation. If following the standard definition [16] one finds such a diffusion coefficient could diverge for deterministic chaotic trajectories, the so-called super- or hyper-diffusion phenomena [19]. One elegant solution is due to Zaslavsky [11] who recognized that the island-chain structure in the phase space of a hamiltonian system (also called stochastic layer) has a fractal dimension in both space and time. Modifying the definition of diffusivity using fractional powers, one can obtain a convergent diffusivity. The resulting Fokker-Planck equation has fractional derivatives in both time and spatial coordinates, hence the name fractional kinetic equation. Novel as it is conceptionally, this approach has not matured to the stage of demonstrating a practical application. Its applicability to highly chaotic flows is also not clear since the surviving islands are usually of negligible size.

### C. Outline of our approach and results

The Lagrangian nature of the chaotic advection and the desire for a solution to advection-diffusion equation in Eulerian frame imply the need for a method that relates the two in the presence of a small but finite diffusivity. A straightforward approach would be to solve the advection-diffusion equation in Lagrangian coordinates, the coordinate system directly associated with the Lagrangian description of fluids. Although the Lagrangian description of a fluid flow is widely known, global Lagrangian coordinates were not applied to the advection-diffusion problem until recently [2]. The validity of this approach is based on the general principle that the description of a physical phenomena is independent of the choice of the coordinate system. The solution in Lagrangian coordinates is non-trivial due to the metric tensor, which arises in the  $\nabla^2$  operator of the diffusion term and is highly anisotropic if the flow is chaotic. The metric tensor rigorously couples the solution of the advection-diffusion equation to the dynamical system theory. It is also the metric tensor that bridges the Lagrangian picture and the Eulerian solution.

One unique feature of the use of global Lagrangian coordinates is the ability to treat flow fields that are far from integrable and thus highly chaotic, an area where less is known but which is of great importance [23]. Although the integrable case is rigorously treated in section VI, we will center our discussion on highly chaotic flows because of their practical importance. By definition, a flow is chaotic if the distance  $\delta$  between neighboring fluid elements tends

to vary (diverge or converge) exponentially in time,  $\delta \propto \delta_0 \exp(\lambda t)$ , with  $\lambda$  the Lyapunov exponent. In advection-diffusion problems, the Lyapunov time  $1/\lambda$  associated with the most negative Lyapunov exponent defines a natural characteristic time scale for a chaotic flow. The characteristic diffusion time  $L^2/D$  is determined by the diffusivity  $D$  and the typical spatial scale  $L$  of the initial gradient of  $\phi$ . Our previous analysis [2] illustrated that the characteristic dimensionless parameter of the chaotic transport problem in two dimensions is the ratio of the characteristic diffusion time and the Lyapunov time of the flow, *i.e.*  $\Omega \equiv \lambda L^2/D$ . The diffusivity is generally very small so  $\Omega \gg 1$ . For  $\Omega \gg 1$  the passive scalar undergoes a pure advection period until the time  $t_a \equiv \ln(2\Omega)/2\lambda$ . A rapid diffusive relaxation removes the spatial gradient of the passive scalar during a period of a few Lyapunov time  $1/\lambda$  centered on the time  $t_a$ . This diffusion is of one dimensional since it only occurs along the  $\hat{\mathbf{s}}_\infty$  direction, which defines the stable direction for neighboring streamlines to converge. In generic flows, the finite time Lyapunov exponent is a function of both time and position. It was found for 2D systems that the geometry of the field line of the  $\hat{\mathbf{s}}_\infty$  vector determines the spatial variation of the finite time Lyapunov exponent along the  $\hat{\mathbf{s}}$  lines, and hence the local diffusive transport [2]. Diffusion is impeded at the sharp bends of an  $\hat{\mathbf{s}}$  line, which has a peculiarly small finite time Lyapunov exponent.

Mixing in a three dimensional flow is clearly important for practical applications. The goal of this paper is to carry out an explicit analysis in 3D and establish a similar level of understanding as previously achieved in 2D [2]. As we will show, the main physics results obtained in 2D apply to 3D situations. These include the characteristic time scales for advection and diffusion which are determined by the Lyapunov time and the dimensionless number  $\Omega$ , and the extreme anisotropy of the diffusive relaxation. Of course, the increase of spatial dimension from two to three does introduce new subtleties in the solution, some of which will be discussed in the main text.

The main body of the paper is organized as follows. Section II gives a description of the problem and an overview of our results, which is the minimum amount of material necessary for understanding the thesis of this paper. In section III, the advection-diffusion equation is solved for a three dimensional flow in natural Lagrangian coordinates. The properties of the finite time Lyapunov exponent and diffusion barriers are discussed in section IV. In section VI transport in an integrable region of a three dimensional flow is treated. Some models of chaotic flows and numerical illustrations are given in section V.

## II. OVERVIEW

Chaos and its effect on diffusive transport in a fluid flow can be conveniently examined using Lagrangian coordinates [25]. The motion of a fluid element is described by the differential equation

$$d\mathbf{x}/dt = \mathbf{v}(\mathbf{x}, t). \quad (4)$$

The trajectory in real space is the solution  $\mathbf{x} = \mathbf{x}(\xi, t)$  with  $\xi = \mathbf{x}(\xi, t = 0)$  the Lagrangian coordinates. The distance between neighboring fluid points at time  $t$  is related to their initial separation by  $d\mathbf{x} \cdot d\mathbf{x} = g_{ij} d\xi^i d\xi^j$ , where  $g_{ij} \equiv (\partial\mathbf{x}/\partial\xi^i) \cdot (\partial\mathbf{x}/\partial\xi^j)$  is the metric tensor of the Lagrangian coordinates. The matrix inverse of  $g_{ij}$  is  $g^{ij} \equiv \nabla\xi^i \cdot \nabla\xi^j$ . The Jacobian of the Lagrangian coordinates is related with the metric tensor by  $J^2 = \|g_{ij}\| = 1/\|g^{ij}\|$ . For a divergence-free flow  $J = 1$ . The metric tensor is a positive definite, symmetric matrix, so it can be diagonalized with real eigenvectors and positive eigenvalues, *i.e.*,

$$g_{ij} = \Lambda_l \hat{\mathbf{e}}\hat{\mathbf{e}} + \Lambda_m \hat{\mathbf{m}}\hat{\mathbf{m}} + \Lambda_s \hat{\mathbf{s}}\hat{\mathbf{s}}$$

with the three positive eigenvalues  $\Lambda_l \geq \Lambda_m \geq \Lambda_s > 0$ . The Lyapunov characteristic exponents of the flow are given by

$$\begin{aligned} \lim_{t \rightarrow \infty} \ln \Lambda_l / 2t &= \lambda_l^\infty, \\ \lim_{t \rightarrow \infty} \ln \Lambda_m / 2t &= \lambda_m^\infty, \\ \lim_{t \rightarrow \infty} \ln \Lambda_s / 2t &= \lambda_s^\infty, \end{aligned}$$

and the eigenvectors  $\hat{\mathbf{e}}$ ,  $\hat{\mathbf{m}}$  and  $\hat{\mathbf{s}}$  have well defined time asymptotic limits:  $\hat{\mathbf{e}}_\infty$ ,  $\hat{\mathbf{m}}_\infty$  and  $\hat{\mathbf{s}}_\infty$  (see appendix A). In those regions where there is a positive Lyapunov exponent, the flow is said to be chaotic, otherwise it is said to be integrable.

For a three dimensional divergence-free flow with symmetry under time reversal, the set of Lyapunov characteristic exponents is symmetric with respect to zero, *i.e.*,  $\lambda_l^\infty = -\lambda_s^\infty = \lambda^\infty > 0$  and  $\lambda_m^\infty = 0$ . The time asymptotic eigenvectors determine the asymptotic behavior of neighboring fluid elements. Along  $\hat{\mathbf{s}}_\infty$  ( $\hat{\mathbf{e}}_\infty$ ) direction, neighboring points converge (diverge) exponentially in time. But their separation varies only algebraically with time along  $\hat{\mathbf{m}}_\infty$

direction. We note that  $\hat{\mathbf{s}}_\infty$  defines the stable direction in a chaotic flow (see appendix A). The  $\hat{\mathbf{s}}_\infty$  is a smooth function of position so it gives rise to a vector field. The field lines of the  $\hat{\mathbf{s}}_\infty$  vector are called  $\hat{\mathbf{s}}$  lines. It should be pointed out that time-dependent flows might not always have the middle Lyapunov exponent zero. Although our analysis is presented in the case of  $\lambda_m = 0$  for the sake of clarity, the more complicated case with an arbitrary combination of positive and negative Lyapunov exponents can also be treated. In fact, a clear understanding of the simple case makes the physics of the more complicated case transparent, for details, see appendix B.

Although the infinite time Lyapunov exponents are better known in mathematics, their finite time analogies are of greater interests in physics. The finite time Lyapunov exponents,

$$\lambda_l(\xi, t) \equiv (\ln \Lambda_l)/2t; \quad \lambda_m(\xi, t) \equiv (\ln \Lambda_m)/2t; \quad \lambda_s(\xi, t) \equiv (\ln \Lambda_s)/2t, \quad (5)$$

are functions of position  $\xi$  and time. We find that the finite time Lyapunov exponent  $\lambda_s$  and its associated  $\hat{\mathbf{s}}_\infty$  vector play the most important role in diffusive transport. This can be seen by transforming the advection-diffusion equation, Eq. (1), into Lagrangian coordinates. For the simplicity of notation, we define

$$\lambda(\xi, t) \equiv -\lambda_s(\xi, t). \quad (6)$$

The inverse of  $\lambda$ ,  $1/\lambda$ , is the Lyapunov time of the flow. We wish to point out again that the most negative Lyapunov exponent ( $\lambda$ ) defines the characteristic Lyapunov time of the flow for advection-diffusion problems.

In Lagrangian coordinates, the advection-diffusion equation becomes an ordinary diffusion equation with a tensor diffusivity  $D^{ij} = Dg^{ij}$  [2],

$$\left(\frac{\partial \phi}{\partial t}\right)_\xi = \frac{1}{\rho_0} \sum \frac{\partial}{\partial \xi^i} \rho_0 D^{ij} \frac{\partial \phi}{\partial \xi^j} \quad (7)$$

where  $\rho_0(\xi)$  is the initial fluid density profile,  $\rho_0(\xi) = \rho(\xi, t=0)$ . The magnitude of the gradient of  $\phi$  is given by

$$(\nabla \phi)^2 = \sum (\partial \phi / \partial \xi^i) g^{ij} (\partial \phi / \partial \xi^j). \quad (8)$$

The effect of the flow on the evolution of a passive scalar is, therefore, determined by the metric tensor of Lagrangian coordinates  $g^{ij}$ . For simplicity we will assume that the initial fluid density distribution  $\rho_0(\xi)$  is a constant. The diffusion equation, Eq. (7), can then be written in Lagrangian coordinates as

$$\partial \phi / \partial t = -\nabla_0 \cdot \gamma \quad \text{with} \quad \gamma \equiv -\overleftrightarrow{\mathbf{D}} \cdot \nabla_0 \phi \quad (9)$$

and  $\overleftrightarrow{\mathbf{D}}$  the tensor diffusivity  $D^{ij}$ . Here  $\nabla_0$  denotes gradient in Lagrangian coordinates. Equation (9) maximizes an entropy-like quantity

$$S \equiv - \int (\phi^2/2) d^3 \xi \quad (10)$$

while holding  $\int \phi d^3 \xi$  constant. The time derivative of  $S$  is

$$dS/dt = - \int (\gamma \cdot \nabla_0 \phi) d^3 \xi. \quad (11)$$

So the entropy production rate per unit volume is positive definite and given by

$$\dot{s}(\xi, t) \equiv -\gamma \cdot \nabla_0 \phi. \quad (12)$$

Only diffusion creates entropy and removes the time reversibility of the system. Even a tiny diffusivity  $D$  leads to an inevitable rapid entropy production in a chaotic flow. To see that, let's substitute  $g^{ij} = \hat{\mathbf{e}}\hat{\mathbf{e}}/\Lambda_l + \hat{\mathbf{m}}\hat{\mathbf{m}}/\Lambda_m + \hat{\mathbf{s}}\hat{\mathbf{s}}/\Lambda_s$  into equation (12),

$$\dot{s} = D(\hat{\mathbf{e}} \cdot \nabla_0 \phi)^2 e^{-2\lambda_l t} + D(\hat{\mathbf{m}} \cdot \nabla_0 \phi)^2 e^{-2\lambda_m t} + D(\hat{\mathbf{s}} \cdot \nabla_0 \phi)^2 e^{2\lambda t}. \quad (13)$$

Since  $\lambda_s < 0$  and  $\lambda \equiv -\lambda_s > 0$ ,  $\dot{s}$  would grow exponentially in time without bound unless the diffusion intervenes and quickly removes the coordinate dependence of  $\phi$  along the  $\hat{\mathbf{s}}$  lines. This result holds independent of the smallness of  $D$ , as long as it does not vanish. Such a conclusion can also be obtained by examining the tensor diffusivity. The effective diffusivity along the  $\hat{\mathbf{e}}_\infty$  direction is negligible since

$$D_{ee} \equiv \hat{\mathbf{e}}_\infty \cdot \overleftrightarrow{\mathbf{D}} \cdot \hat{\mathbf{e}}_\infty \approx D / \exp(2\lambda_l t)$$

with  $\lambda_l > 0$ . The effective diffusivity along the  $\hat{\mathbf{m}}_\infty$  direction

$$D_{mm} \equiv \hat{\mathbf{m}}_\infty \cdot \overleftrightarrow{\mathbf{D}} \cdot \hat{\mathbf{m}}_\infty \approx D/\Lambda_m$$

is small if  $D$  is small. In contrast, the effective diffusivity along the  $\hat{\mathbf{s}}_\infty$  direction grows exponentially in time,

$$D_{ss} \equiv \hat{\mathbf{s}}_\infty \cdot \overleftrightarrow{\mathbf{D}} \cdot \hat{\mathbf{s}}_\infty \approx D/\Lambda_s \approx D \exp(2\lambda t).$$

The exponential amplification of the effective diffusivity along the  $\hat{\mathbf{s}}_\infty$  direction in Lagrangian coordinates corresponds to an exponentially growing gradient of the passive scalar in real space. It is easy to see that the diffusion becomes a dominant process in a chaotic flow for  $\lambda t \gg 1$  regardless of how small  $D$  may be. Furthermore, the diffusion, once it becomes important, is highly anisotropic.

The strong anisotropy of the diffusion process demands care in the choice of coordinates. The rapid diffusion, which occurs only along an  $\hat{\mathbf{s}}$  line, can be confined to one coordinate if the coordinate system is chosen appropriately. We named such coordinate system natural Lagrangian coordinates [24] and showed how to construct them in 2D in [2]. In this paper, we give a form of natural Lagrangian coordinates in three dimensional space, which then allows us to obtain the general properties of the solution to the advection-diffusion equation in a three dimensional chaotic flow. The findings agree with our earlier results in 2D [2]. In summary, the characteristic dimensionless parameter  $\Omega$  for the chaotic transport of a passive scalar is the ratio of the characteristic diffusion time and the Lyapunov time of the flow,

$$\Omega \equiv \lambda L^2/D, \quad (14)$$

with  $L$  the typical spatial scale and  $\lambda$  the Lyapunov exponent, equation (6). If the characteristic diffusion time  $L^2/D$  is much longer than the Lyapunov time  $1/\lambda$  of the flow, *i.e.*,  $\Omega \gg 1$ , the chaotic transport is given by ideal advection (the scalar is carried by the fluid element along its trajectory) for time less than  $t_a - 1/2\lambda$  with  $t_a \equiv (\ln 2\Omega)/2\lambda$ . The ideal advection causes the gradient of the scalar field to increase by a factor of  $\Omega$ . Then a rapid diffusion occurs and causes the flattening of the gradient and associated entropy production during a relatively short interval  $1/\lambda$  centered on  $t_a$ . This rapid diffusive relaxation occurs only along the  $\hat{\mathbf{s}}$  lines, which is a special feature for chaotic flows.

The existence of a characteristic chaotic transport time scale  $t_a$  implies that the finite time Lyapunov exponent rather than the infinite time Lyapunov exponent determines the chaotic transport. The spatio-temporal complexity of the diffusive transport, as reflected in the entropy production rate per unit volume  $\dot{s}$ , is determined by the finite time Lyapunov exponent  $\lambda(\xi, t)$ . For example, the places with significantly smaller  $\lambda(\xi, t)$  (hence  $\Omega$ ) pose barriers for the diffusive transport and entropy production. It must be emphasized that once the flow field is specified, the finite time Lyapunov exponent  $\lambda(\xi, t)$  is completely determined.

Numerical results suggest that the finite time Lyapunov exponent  $\lambda(\xi, t)$  of a three dimensional conservative system can be decomposed into three parts,

$$\lambda(\xi, t) = \tilde{\lambda}(\xi)/t + f(\xi, t)/\sqrt{t} + \lambda^\infty, \quad (15)$$

where

$$\hat{\mathbf{s}}_\infty \cdot \nabla_0 f(\xi, t) = 0 \quad (16)$$

and  $\lambda^\infty$  is the infinite time Lyapunov exponent. The spatial dependence of the finite time Lyapunov exponent  $\lambda(\xi, t)$  is related to the geometry of the  $\hat{\mathbf{s}}$  line through  $\tilde{\lambda}$  by

$$\hat{\mathbf{s}}_\infty \cdot \nabla_0 \tilde{\lambda}(\xi) + \nabla_0 \cdot \hat{\mathbf{s}}_\infty = 0, \quad (17)$$

where  $\tilde{\lambda}(\xi)$  is a smooth function of position due to the smoothness of the vector field  $\hat{\mathbf{s}}_\infty$ . Hence we have, once again, directly related the geometry of an  $\hat{\mathbf{s}}$  line to the diffusive transport through  $\lambda(\xi, t)$ . These new results for three dimensional systems, equations (15,16,17), have the exactly same form as what we found for two dimensional conservative systems [2] [of course, the number of spatial coordinates is now three in equation (17)]. Just like in 2D, the function  $\tilde{\lambda}$  in equation (15) is responsible for the description of barriers for diffusive transport in chaotic flows while the function  $f(\xi, t)$  characterizes the fractal nature of the chaotic advection [8,22] and the chaotic diffusive transport [2].

Fast diffusion occurs along the  $\hat{\mathbf{s}}$  lines and entropy production rate  $\dot{s}$  is given by the finite time Lyapunov exponent  $\lambda(\xi, t)$ . Equations (15,16,17) imply that  $\lambda(\xi, t)$  varies little if the  $\hat{\mathbf{s}}$  line is straight (hence small  $\nabla_0 \cdot \hat{\mathbf{s}}_\infty$ ). But  $\lambda(\xi, t)$  will have a strong variation where the  $\hat{\mathbf{s}}$  line has a sharp bend. Our numerical results show that  $\lambda(\xi, t)$  makes a sharp

dip at the sharp bends of the  $\hat{\mathbf{s}}$  lines, for an illustration, see figure 8. Small  $\lambda$  leads to a small  $\Omega$ . Hence diffusive transport is impeded on the sharp bends of the  $\hat{\mathbf{s}}$  lines and a class of diffusion barriers is created inside the chaotic region of the flow. Our results on diffusion barriers in 2D chaotic flows, therefore, have been reestablished in three dimensional flows.

We find that there are also spatially separated fast diffusion and slow diffusion in an integrable region of a shear flow. The fast diffusion is confined to the KAM surfaces only, while the slow diffusion occurs across the good KAM surfaces. It is the radial direction across the nested KAM surfaces in which a significant gradient of the scalar field can be maintained. For a detailed analysis, see section VI.

### III. SOLVING THE ADVECTION-DIFFUSION EQUATION IN NATURAL LAGRANGIAN COORDINATES

The tensor diffusivity  $Dg^{ij}$  with  $g^{ij} = \Lambda_l^{-1}\hat{\mathbf{e}}\hat{\mathbf{e}} + \Lambda_m^{-1}\hat{\mathbf{m}}\hat{\mathbf{m}} + \Lambda_s^{-1}\hat{\mathbf{s}}\hat{\mathbf{s}}$  is strongly anisotropic due to the chaotic nature of the flow. By introducing a set of new Lagrangian coordinates in which the large component of diffusion affects only one coordinate, we can simplify the computation and understand the general properties of the chaotic transport of passive scalars. A coordinate system that has this property is called natural Lagrangian coordinates [24].

In two dimensions, the metric tensor is  $g^{ij} = \Lambda_l^{-1}\hat{\mathbf{e}}\hat{\mathbf{e}} + \Lambda_s^{-1}\hat{\mathbf{s}}\hat{\mathbf{s}}$ , and the curl of  $\hat{\mathbf{e}}_\infty$  and  $\hat{\mathbf{s}}_\infty$  will be orthogonal to themselves. That is, if we write  $\hat{\mathbf{e}}_\infty = e_x\hat{\mathbf{x}} + e_y\hat{\mathbf{y}}$  and  $\hat{\mathbf{s}}_\infty = s_x\hat{\mathbf{x}} + s_y\hat{\mathbf{y}}$ , the curls will lie along the  $\hat{\mathbf{z}}$  axis. Hence natural Lagrangian coordinates  $\alpha$ - $\beta$  can be defined by  $\hat{\mathbf{e}}_\infty = a\nabla\alpha$  and  $\hat{\mathbf{s}}_\infty = b\nabla\beta$  with Jacobian  $J_{\alpha\beta} = ab$  [2], using the orthonormality of  $\hat{\mathbf{e}}_\infty$  and  $\hat{\mathbf{s}}_\infty$ ,  $\hat{\mathbf{s}}_\infty \cdot \nabla\alpha = 0$  and  $\hat{\mathbf{e}}_\infty \cdot \nabla\beta = 0$ .

In three dimensions, we can establish  $\alpha$ - $\beta$ - $\zeta$  coordinates such that  $\hat{\mathbf{s}}_\infty \cdot \nabla\alpha = \hat{\mathbf{s}}_\infty \cdot \nabla\zeta = 0$ , but in general one can not choose the other coordinate  $\beta$  such that  $\hat{\mathbf{e}}_\infty \cdot \nabla\beta = \hat{\mathbf{m}}_\infty \cdot \nabla\beta = 0$ . To separate out the large component of diffusion, the  $\hat{\mathbf{s}}_\infty$  vector must satisfy  $\hat{\mathbf{s}}_\infty \cdot \nabla\alpha = 0$  and  $\hat{\mathbf{s}}_\infty \cdot \nabla\zeta = 0$ . The coordinates  $\alpha$ - $\beta$ - $\zeta$  given by the following equations

$$\begin{aligned}\nabla\alpha &= f\hat{\mathbf{e}}_\infty + g\hat{\mathbf{m}}_\infty \\ \nabla\zeta &= p\hat{\mathbf{e}}_\infty + q\hat{\mathbf{m}}_\infty \\ \nabla\beta &= a\hat{\mathbf{e}}_\infty + b\hat{\mathbf{m}}_\infty + c\hat{\mathbf{s}}_\infty\end{aligned}\tag{18}$$

satisfy this requirement. The functions  $f, g, p, q, a, b$  and  $c$  are determined locally by the properties of  $\hat{\mathbf{e}}_\infty$ ,  $\hat{\mathbf{m}}_\infty$  and  $\hat{\mathbf{s}}_\infty$  from a set of first order differential equations (for a proof that such a coordinate system exists in the neighborhood of an arbitrary point, see appendix C). The Jacobian of the  $\alpha$ - $\beta$ - $\zeta$  coordinates is  $J_n = 1/(fq - gp)c$ . In both 2D and 3D cases, the  $\beta$  coordinate gives the direction of rapid diffusion. Diffusion in the other coordinate(s) is either severally suppressed or can not be distinguished from that in an integrable flow.

The infinite time Lyapunov exponent is a constant in one ergodic region. The finite time Lyapunov exponents, as defined in equation (5), are functions of position and time. The eigenvectors of the metric tensor  $\hat{\mathbf{e}}$ ,  $\hat{\mathbf{m}}$  and  $\hat{\mathbf{s}}$  also depend on position and time. They converge to time independent functions of Lagrangian position, the time asymptotic eigenvectors  $\hat{\mathbf{e}}_\infty(\xi)$ ,  $\hat{\mathbf{m}}_\infty(\xi)$  and  $\hat{\mathbf{s}}_\infty(\xi)$ , for  $\Lambda_s^{-1} \gg 1$ . The convergence of the  $\hat{\mathbf{s}}$  vector is of most importance, and the finite time  $\hat{\mathbf{s}}$  is related to the asymptotic eigenvectors by

$$\hat{\mathbf{s}} \propto \hat{\mathbf{s}}_\infty + \sigma_m\Lambda_s\hat{\mathbf{m}}_\infty + \sigma_e\Lambda_s\hat{\mathbf{e}}_\infty\tag{19}$$

where  $\sigma_m(t)$  and  $\sigma_e(t)$  depend algebraically on time and measure the rate of convergence, for a numerical illustration see Fig. 1 in section V.

The  $\alpha$ - $\beta$ - $\zeta$  coordinate system with Jacobian  $J_n = 1/(fq - gp)c$  simplifies the diffusion equation, Eq. (9). In these coordinates one has

$$\frac{\partial\phi}{\partial t} = -\frac{1}{J_n}\frac{\partial}{\partial\alpha}(J_n\gamma^\alpha) - \frac{1}{J_n}\frac{\partial}{\partial\beta}(J_n\gamma^\beta) - \frac{1}{J_n}\frac{\partial}{\partial\zeta}(J_n\gamma^\zeta)\tag{20}$$

where  $\gamma^\alpha, \gamma^\beta$  and  $\gamma^\zeta$  are the fluxes in the  $\alpha, \beta$  and  $\zeta$  directions,

$$\gamma^\alpha = -D_{\alpha\alpha}\frac{\partial\phi}{\partial\alpha} - D_{\alpha\beta}\frac{\partial\phi}{\partial\beta} - D_{\alpha\zeta}\frac{\partial\phi}{\partial\zeta}\tag{21}$$

$$\gamma^\beta = -D_{\beta\alpha}\frac{\partial\phi}{\partial\alpha} - D_{\beta\beta}\frac{\partial\phi}{\partial\beta} - D_{\beta\zeta}\frac{\partial\phi}{\partial\zeta}\tag{22}$$

$$\gamma^\zeta = -D_{\zeta\alpha}\frac{\partial\phi}{\partial\alpha} - D_{\zeta\beta}\frac{\partial\phi}{\partial\beta} - D_{\zeta\zeta}\frac{\partial\phi}{\partial\zeta},\tag{23}$$

with

$$D_{\alpha\alpha} = f^2 D_{ee} + g^2 D_{mm} + 2fg D_{em} \quad (24)$$

$$D_{\beta\beta} = a^2 D_{ee} + b^2 D_{mm} + c^2 D_{ss} + 2ab D_{em} + 2ac D_{es} + 2bc D_{ms} \quad (25)$$

$$D_{\zeta\zeta} = p^2 D_{ee} + q^2 D_{mm} + 2pq D_{em} \quad (26)$$

$$D_{\alpha\beta} = D_{\beta\alpha} = af D_{ee} + (bf + ag) D_{em} + bg D_{mm} + cf D_{es} + cg D_{ms} \quad (27)$$

$$D_{\zeta\beta} = D_{\beta\zeta} = ap D_{ee} + (bp + aq) D_{em} + bq D_{mm} + cp D_{es} + cq D_{ms} \quad (28)$$

$$D_{\alpha\zeta} = D_{\zeta\alpha} = fp D_{ee} + gq D_{mm} + (fq + gp) D_{em}. \quad (29)$$

The diffusion coefficients are

$$D_{ee} \equiv \hat{\mathbf{e}}_\infty \cdot \overleftrightarrow{\mathbf{D}} \cdot \hat{\mathbf{e}}_\infty; \quad D_{em} \equiv \hat{\mathbf{e}}_\infty \cdot \overleftrightarrow{\mathbf{D}} \cdot \hat{\mathbf{m}}_\infty; \quad D_{mm} \equiv \hat{\mathbf{m}}_\infty \cdot \overleftrightarrow{\mathbf{D}} \cdot \hat{\mathbf{m}}_\infty; \quad (30)$$

$$D_{se} \equiv \hat{\mathbf{s}}_\infty \cdot \overleftrightarrow{\mathbf{D}} \cdot \hat{\mathbf{e}}_\infty; \quad D_{sm} \equiv \hat{\mathbf{s}}_\infty \cdot \overleftrightarrow{\mathbf{D}} \cdot \hat{\mathbf{m}}_\infty; \quad D_{ss} \equiv \hat{\mathbf{s}}_\infty \cdot \overleftrightarrow{\mathbf{D}} \cdot \hat{\mathbf{s}}_\infty. \quad (31)$$

In this set of natural Lagrangian coordinates, the anisotropic properties of the metric tensor are inherited by the diffusive flux in different coordinate directions, *i.e.*,  $\gamma^\beta \gg \gamma^\alpha$  or  $\gamma^\zeta$ . This can be illustrated by considering a chaotic divergence-free flow in which  $\lambda_l^\infty = -\lambda_s^\infty = \lambda$  and  $\lambda_m^\infty = 0$ . Substituting  $g^{ij} = \exp(-2\lambda_l t) \hat{\mathbf{e}} \hat{\mathbf{e}} + \exp(-2\lambda_m t) \hat{\mathbf{m}} \hat{\mathbf{m}} + \exp(-2\lambda_s t) \hat{\mathbf{s}} \hat{\mathbf{s}}$  into the tensor diffusivity and using the orthonormality of  $\hat{\mathbf{e}}$ ,  $\hat{\mathbf{m}}$ , and  $\hat{\mathbf{s}}$ , we find that the diffusion coefficients satisfy the inequalities  $D_{ee} \approx D_{em} \approx D \exp(-2\lambda t) \ll D_{mm} \approx D \leq D_{es} \approx D \sigma_e (D_{ms} \approx D \sigma_m) \ll D_{ss} \approx D \exp(2\lambda t)$  for  $\Lambda_l \approx \Lambda_s^{-1} \gg 1$ . Consequently,  $D_{\beta\beta} \approx D \exp(2\lambda t)$  is much greater than  $D_{\alpha\alpha}$ ,  $D_{\zeta\zeta}$ ,  $D_{\alpha\beta}$ ,  $D_{\zeta\beta}$ , and  $D_{\alpha\zeta}$  which are at most bounded by  $D\sigma$ ,  $\sigma = \sup(\sigma_e, \sigma_s)$ , for  $\Lambda_l \approx \Lambda_s^{-1} \gg 1$ .

The diffusion in a chaotic flow is one-dimensional. This remarkable property of equation (20) can be illustrated by an exact solution for a chaotic flow modeled by a trivial extension of Arnold's cat map [39],

$$x_{n+1} = x_n + y_n; \quad y_{n+1} = x_n + 2y_n; \quad z_{n+1} = z_n.$$

It is easy to check that  $g^{ij} = \Lambda^{-1} \hat{\mathbf{e}}_\infty \hat{\mathbf{e}}_\infty + \hat{\mathbf{m}}_\infty \hat{\mathbf{m}}_\infty + \Lambda \hat{\mathbf{s}}_\infty \hat{\mathbf{s}}_\infty$ ,  $\lambda = (\ln \Lambda)/2t$  a constant, and  $f = q = c = 1$ ,  $g = p = a = b = 0$ . The diffusion equation (20) now takes the simple form

$$\frac{\partial \phi}{\partial t} = -D \exp(-2\lambda t) \frac{\partial^2 \phi}{\partial \alpha^2} - D \frac{\partial^2 \phi}{\partial \zeta^2} - D \exp(2\lambda t) \frac{\partial^2 \phi}{\partial \beta^2}$$

This equation can be solved straightforwardly by the method of separation of variables. As an example, for such a flow in an infinitely extended space an initial distribution of the scalar field  $\phi(t=0) = c_0(1 - \cos k\alpha)(1 - \cos k\beta)(1 - \cos k\zeta)$  relaxes as

$$\begin{aligned} \phi = c_0 \{ & 1 - \exp[-(1 - e^{-2\lambda t})/2\Omega] \cos k\alpha \} \\ & \{ 1 - \exp[-(e^{2\lambda t} - 1)/2\Omega] \cos k\beta \} \\ & \{ 1 - \exp(-Dk^2 t) \cos k\zeta \} \end{aligned} \quad (32)$$

with  $\Omega = \lambda/k^2 D$  the ratio of the characteristic diffusion time of the passive scalar ( $1/k^2 D$ ) and the Lyapunov time of the flow ( $1/\lambda$ ). One might be concerned that the construction of  $\hat{\mathbf{s}}$  lines and finite time Lyapunov exponents in the example was based on a map but the solution was given in the continuous time. There are two ways to interpret this result, neither affects the essential physics. One is to regard equation (32) as the solution for a time periodic flow field which has the form of the cat map if sampled at the periods of the flow. This is justified since the map and the flow field from which it is reduced have the same spatial dependence of the  $\hat{\mathbf{s}}$  lines and finite time Lyapunov exponents in Lagrangian coordinates. In the other approach one simply interprets equation (32) as the diffusive relaxation for a map by taking  $t$  at discrete time intervals. We also note that a solution of similar form to equation (32) was given in [28] to illustrate the effect of turbulent strains on the small scale variation of passive scalars.

The solution has distinct characteristic dependence in the different coordinate directions. For  $\Omega \gg 1$ , the function  $\phi$  retains its initial  $\alpha$  dependence. For  $t < t_a - 1/2\lambda$  with  $t_a \equiv \ln(2\Omega)/2\lambda$  the solution is accurately approximated by the initial distribution  $\phi_0$ . The  $\beta$  dependence of  $\phi$  is damped during a short interval  $1/\lambda$  centered on the time  $t = t_a$ . Despite  $\phi$  retaining its initial  $\alpha$  dependence,  $(\partial\phi/\partial\alpha)g^{\alpha\alpha}(\partial\phi/\partial\alpha)$  becomes small for  $t$  greater than  $t_a$  due to the smallness of the  $g^{\alpha\alpha}$  component of the metric tensor. The asymptotic form for the gradient of  $\phi$  is determined by the slow varying  $\zeta$  dependence,  $(\nabla\phi)^2 \approx (\nabla\phi_0)^2 \exp(-2t/\tau_d)$  with  $\tau_d = 1/Dk^2$  the characteristic diffusion time. Hence it is no different from that of an integrable flow.

This can also be shown by examining the rate of the production of entropy-like quantity  $S$  which was defined in equation (10). In natural Lagrangian coordinates



$$\begin{aligned} \frac{dS}{dt} = \int & \left[ \frac{1}{D_{\beta\beta}} (\gamma^\beta)^2 + \left( D_{\alpha\alpha} - \frac{D_{\alpha\beta}^2}{D_{\beta\beta}} \right) \left( \frac{\partial\phi}{\partial\alpha} \right)^2 + \left( D_{\zeta\zeta} - \frac{D_{\beta\zeta}^2}{D_{\beta\beta}} \right) \left( \frac{\partial\phi}{\partial\zeta} \right)^2 \right. \\ & \left. + 2 \left( D_{\alpha\zeta} - \frac{D_{\alpha\beta} D_{\beta\zeta}}{D_{\beta\beta}} \right) \frac{\partial\phi}{\partial\alpha} \frac{\partial\phi}{\partial\zeta} \right] J_n d\alpha d\beta d\zeta. \end{aligned} \quad (33)$$

The  $(\gamma^\beta)^2$  (the diffusive flux in  $\beta$  coordinate) gives the main pulse of  $S$  production in the time interval  $1/\lambda$  centered on the time  $t_a$ . On a longer time scale, this term and the  $(\partial\phi/\partial\alpha)^2$  term give an  $S$  production that scales as  $\exp(-2\lambda t)$ , while the  $(\partial\phi/\partial\zeta)^2$  term makes the dominate contribution which scales as  $\exp(-2t/\tau_d)$  with  $\tau_d = 1/Dk^2$  the characteristic diffusion time.

In 3D flows the  $\hat{\mathbf{e}}_\infty$  and  $\hat{\mathbf{m}}_\infty$  vectors are generally mixed in natural Lagrangian coordinates  $\alpha$  and  $\zeta$ . Consequently, diffusion in these two coordinate directions are dominated by the contribution from  $\hat{\mathbf{m}}$  direction and they have the characteristic time scale of an integrable flow, just like the  $\zeta$  dependence of  $\phi$  in Eq. (32). It is the diffusion in the  $\beta$  coordinate that distinguishes the transport of a passive scalar in a chaotic flow from that in an integrable flow.

The  $\hat{\mathbf{s}}$  lines give the most important information for constructing the natural Lagrangian coordinate system, and thus determine the evolution of a passive scalar. A single  $\hat{\mathbf{s}}$  line generically fills a chaotic region in bounded systems. This implies that the asymptotic (*i.e.*, on the time scale which is much longer than the typical advection time) evolution of the passive scalar in a generic chaotic flow is different from that of the simplified solution given earlier, Eq. (32). That is, the final  $\phi$  distribution will not retain any coordinate dependence in the region where the flow field is chaotic and the smoothing of the gradient of  $\phi$  scales at a rate much faster than  $\nabla\phi_0 \exp(-t/\tau_d)$  with  $\tau_d = L^2/D$  the characteristic diffusion time.

It should be noted that the simple model based on cat map is mixing in the  $x$ - $y$  plane and has straight  $\hat{\mathbf{s}}$  lines due to hyperbolicity. Generic flows are only ergodic and can have non-hyperbolic points. In other words, generic flows can have integrable regions and their  $\hat{\mathbf{s}}$  lines have a complicated geometry. The next two sections study the additional features of the properties of the solution to the advection-diffusion equation which were missing from the simple model flow based on cat map.

#### IV. FINITE TIME LYAPUNOV EXPONENT AND BARRIERS FOR DIFFUSION

Unlike the infinite time Lyapunov exponent which is a constant in one chaotic zone, the finite time Lyapunov exponent for any given time  $\lambda(\xi, t_0)$  can, and generally does, vary significantly over space for a generic chaotic flow. The strong spatial dependence of the finite time Lyapunov exponent produces a large spread in the time during which diffusion is important. Such effect can be examined both crudely and exactly, corresponding to a study of the statistical properties and the exact spatial dependence of the finite time Lyapunov exponent, respectively.

To understand the termination of the enhanced diffusive transport at a crude level, one can convolute the time  $t_a$  with the corresponding probability distribution function of the finite time Lyapunov exponent. The probability distribution of the finite time Lyapunov exponents  $\lambda(\xi, t = t_0) \equiv -\ln \Lambda_s(\xi, t = t_0)/2t_0$  is approximately Gaussian with respect to variation in space, so will be the spread in time  $t_a$ . Since the difference between the distribution of the finite time Lyapunov exponents and a Gaussian distribution becomes smaller as one samples the finite time Lyapunov exponent at a longer time interval (larger  $t_0$ ), the spread in  $t_a$  becomes more Gaussian-like for systems with longer characteristic diffusion time scale  $L^2/D$ . Furthermore, the spread in the time during which the main entropy pulse occurs is small if the characteristic diffusion time is long. This is due to the fact that the standard deviation of the distribution of the finite time Lyapunov exponent scales as  $1/\sqrt{t_0}$ . Numerical illustration of these properties are given in Figs. 2-5 in section V.

A detailed examination of the diffusive transport requires the knowledge of the exact spatial-temporal dependence of the finite time Lyapunov exponent in a given chaotic flow, especially the spatial variation of  $\lambda(\xi, t)$  along the  $\hat{\mathbf{s}}$  lines, since that is the line along which the rapid diffusive relaxation occurs. These information are given by equations (15,16,17). In [2] we derived equations (15,16,17) for two dimensional conservative systems by applying the constraint that the Riemann-Christoffel curvature tensor must vanish in a flat space on which the Lagrangian coordinates are defined. A similar calculation in 3D is currently not feasible, so we instead resort to a numerical resolution.

The key to equations (15,16,17) is to show

$$\lim_{t \rightarrow \infty} [\hat{\mathbf{s}}_\infty(\xi) \cdot \nabla_0 \lambda(\xi, t)t + \nabla_0 \cdot \hat{\mathbf{s}}_\infty(\xi)] = 0. \quad (34)$$

Once this relationship is established, one can immediately see that  $\lim_{t \rightarrow \infty} \hat{\mathbf{s}}_\infty \cdot \nabla_0 \lambda(\xi, t)t$  can not have a time dependence. Let

$$\lim_{t \rightarrow \infty} \hat{\mathbf{s}}_\infty \cdot \nabla_0 \lambda(\xi, t)t = \hat{\mathbf{s}}_\infty \cdot \nabla_0 \tilde{\lambda}(\xi) \quad (35)$$

with  $\tilde{\lambda}$  a time independent smooth function of position. Equation (35) allows a function  $f(\xi, t)$  satisfying

$$\hat{\mathbf{s}}_\infty \cdot \nabla_0 f(\xi, t) = 0 \quad (36)$$

to be included in the decomposition of  $\lambda(\xi, t)$ . The function  $f(\xi, t)$  is bounded by a  $\sqrt{t}$  dependence in equation (15). The obvious reason is that  $\lim_{t \rightarrow \infty} f(\xi, t)/\sqrt{t}$  has to vanish to satisfy the definition  $\lim_{t \rightarrow \infty} \lambda(\xi, t) = \lambda^\infty$ . The exact choice of  $\sqrt{t}$  comes from the fact that the standard deviation of the distribution of the finite time Lyapunov exponent over space has a  $1/\sqrt{t}$  dependence. Deviation from this  $1/\sqrt{t}$  dependence at finite time is captured by the weak time dependence in  $f(\xi, t)$ .

We have numerically evaluated

$$\Delta(\xi, t) \equiv |\hat{\mathbf{s}} \cdot \nabla_0 \lambda_0 t + \nabla_0 \cdot \hat{\mathbf{s}}| \quad (37)$$

for two different models of three dimensional flows, section V. Similar as what we did in [2], a finite difference scheme is avoided by expressing  $\Delta(\xi, t)$  in terms of the spatial derivatives of the metric tensor, appendix E. We find that  $\Delta(\xi, t)$  converges exponentially in time to zero. The convergence rate is approximately equal to that of the  $\hat{\mathbf{s}}$  vector, *i.e.*, twice the Lyapunov exponent, as can be seen in Fig. 6 in section V. Hence we have numerically validated equation (34), which is the basis for equations (15,16,17).

The spatial derivative of the finite time Lyapunov exponent along an  $\hat{\mathbf{s}}$  line is proportional to the divergence of the  $\hat{\mathbf{s}}_\infty$  vector. For straight segments of an  $\hat{\mathbf{s}}$  line, the divergence of  $\hat{\mathbf{s}}_\infty$  is small, so is the variation in the finite time Lyapunov exponent. At the sharp bends of an  $\hat{\mathbf{s}}$  line, the finite time Lyapunov exponent makes a large swing in its magnitude in accordance with the large oscillation of  $\nabla \cdot \hat{\mathbf{s}}_\infty$ . Analytically speaking, the finite time Lyapunov exponent attains a local minimum along an  $\hat{\mathbf{s}}$  line where

$$\nabla \cdot \hat{\mathbf{s}}_\infty = 0 \quad \text{and} \quad \hat{\mathbf{s}}_\infty \cdot \nabla(\nabla \cdot \hat{\mathbf{s}}_\infty) < 0$$

and reaches a local maximum along an  $\hat{\mathbf{s}}$  line where

$$\nabla \cdot \hat{\mathbf{s}}_\infty = 0 \quad \text{and} \quad \hat{\mathbf{s}}_\infty \cdot \nabla(\nabla \cdot \hat{\mathbf{s}}_\infty) > 0.$$

In terms of simple geometry, the finite time Lyapunov exponent has a maximum where the neighboring  $\hat{\mathbf{s}}$  lines are squeezed and has a minimum where the neighboring  $\hat{\mathbf{s}}$  lines are bulged outward. In the cases that we have studied, the finite time Lyapunov exponent has a sharp dip at the sharp bends of an  $\hat{\mathbf{s}}$  line. The bending of an  $\hat{\mathbf{s}}$  line can be characterized by its local curvature. In 3D, the curvature of the  $\hat{\mathbf{s}}$  lines has an  $\hat{\mathbf{e}}$  and an  $\hat{\mathbf{m}}$  component. Figure 8 shows the variation of the finite time Lyapunov exponent along an  $\hat{\mathbf{s}}$  line and the variation of the  $\hat{\mathbf{s}}$  line curvature.

The equations (15,16,17) have a surprisingly broad range of applications. It uncovers a direct link between the finite time Lyapunov exponent and the  $\hat{\mathbf{s}}_\infty$  vector field. (Note:  $\hat{\mathbf{s}}_\infty$  labels the stable direction, it is the tangent vector of the local stable manifold if the latter exists. The  $\hat{\mathbf{s}}$  line is equivalent to the Lagrangian stable foliation in a general time dependent flow.) By relating geometry ( $\hat{\mathbf{s}}$  lines) to a dynamical quantity (Lyapunov exponent), it provides new insights into the understanding of chaotic systems in general and hamiltonian systems in particular [21]. The importance of this discovery in transport study is transparent. It forms the basis for a detailed examination of diffusive transport in a chaotic flow. As shown in the last section, the rapid diffusion only occurs along the  $\hat{\mathbf{s}}$  lines. According to equations (15,16,17) the finite time Lyapunov exponent and hence the characteristic dimensionless parameter  $\Omega$  vary little on a segment of the  $\hat{\mathbf{s}}$  lines which is straight (small  $\nabla_0 \cdot \hat{\mathbf{s}}_\infty$ ). Consequently the spatial gradient of the passive scalar on a straight  $\hat{\mathbf{s}}$  line segment would be wiped out by a rapid diffusion during a short duration. The situations are quite different on the two ends of this straight  $\hat{\mathbf{s}}$  line segment, which are identified as the sharp bends of the  $\hat{\mathbf{s}}$  line. The finite time Lyapunov exponent has a sharp variation in its magnitude at these sharp bends of the  $\hat{\mathbf{s}}$  lines. Numerical results have consistently shown a sharp drop in the magnitude of the finite time Lyapunov exponent, see section V. A peculiarly small  $\lambda$  leads to a significant reduction in  $\Omega$ , hence a form of local diffusion barrier is created. A simple analogy is the temperature relaxation in a line of iron rods bound together by some plastic chips. The temperature gradient will be removed in each iron rod very quickly but the plastic chips would serve as a practical thermal barrier on this fast time scale. Of course, the whole system will reach to thermal equilibrium after certain time if the system is isolated from the surroundings. The exact time scale for this to happen is given by the thermal conductivity of the plastic chips.

The existence of diffusion barriers associated with the sharp bends of the  $\hat{\mathbf{s}}$  lines actually remedies a pathology of the natural Lagrangian coordinates in applications. The natural Lagrangian coordinates defined in last section are intrinsically local coordinates. Natural Lagrangian coordinates are closely related to the Clebsch coordinates (see appendix C). It is well known that the Clebsch coordinates, which are also called Euler potentials, are not generally single-valued if one attempts to extend them over large regions [29]. However, this pathology is not as important as

it first appears since the presence of local diffusion barriers along the  $\hat{\mathbf{s}}$  line effectively impose boundary conditions in the natural Lagrangian coordinates, and hence only local coordinates are relevant for describing the chaotic transport which has well separated time scales.

If not for the second term  $f(\xi, t)/\sqrt{t}$  in equation (15), the finite time Lyapunov exponent would be a smooth function in space for arbitrary time. In fact, the finite time Lyapunov exponent becomes a fractal function of position across the  $\hat{\mathbf{s}}$  lines for large  $t$ , since  $f(\xi, t)$  develops an exponentially growing spatial gradient in time along directions away from the  $\hat{\mathbf{s}}_\infty$  direction [2].

For any given time  $t_0$ , this property is reflected in the correlation length of the finite time Lyapunov exponent in different directions. The correlation length along the  $\hat{\mathbf{s}}$  line is extremely long since  $\lambda$  is a smooth function along this direction. Across the  $\hat{\mathbf{s}}$  line, the irregularity in  $f(\xi, t_0)$  overwhelms the regularity in  $\lambda$  and the correlation length for  $\lambda$  is greatly reduced. The richest structure and hence the shortest correlation length, lies along the  $\hat{\mathbf{e}}$  lines. The fractal nature of function  $f(\xi, t)$  brings another degree of complexity to the diffusive relaxation. That is, the entropy production in a chaotic flow is a fractal function of space and time. In retrospect, the spread in the time during which the main entropy production pulse occurs is actually determined by  $f(\xi, t)$ , since the standard deviation  $\sigma(t)$  of the distribution of finite time Lyapunov exponents is given by

$$\sigma(t) = (\sqrt{\langle f^2 \rangle - \langle f \rangle^2 / \lambda^\infty}) t^{-1/2} + O(t^{-1}), \quad (38)$$

where  $\langle \dots \rangle$  denotes averaging over space.

## V. FLOW MODELS AND NUMERICAL ILLUSTRATION

To examine the transport problem quantitatively, one has to model the chaotic flow. For simplicity, we have used area(volume)-preserving maps to model a divergence-free flow. The standard map (SM) [39]

$$\begin{aligned} x_{n+1} &= x_n - (k/2\pi) \sin(2\pi y_n) \\ y_{n+1} &= y_n + x_{n+1}, \end{aligned} \quad (39)$$

with  $k$  a constant, is a good choice for modeling a 2D time-periodic divergence-free flow. We have devised an extended 3D version of the standard map (ESM)

$$\begin{aligned} x_{n+1} &= x_n - (k/2\pi) \sin(2\pi y_n) + \Delta \\ y_{n+1} &= y_n - z_n \\ z_{n+1} &= y_n - x_{n+1} \end{aligned} \quad (40)$$

with  $k$  and  $\Delta$  constants, to model a 3D divergence-free flow. ESM is attractive for studying chaotic advection-diffusion problem since it is a divergence-free map based on well-studied standard map and a point spirals along a KAM surface much the same as the motion of a fluid element trapped in a fluid vortex.

The ABC flow  $\mathbf{v} = (v_x, v_y, v_z)$  is another example of a three dimensional divergence-free flow [30,11],

$$\begin{aligned} v_x &= A \sin z + C \cos y; \\ v_y &= B \sin x + A \cos z; \\ v_z &= C \sin y + B \cos x. \end{aligned} \quad (41)$$

It satisfies the Beltrami condition  $\nabla \times \mathbf{v} = \mathbf{v}$  and allows chaotic stream lines. The ABC flow has direct relevance in hydrodynamics since it is a solution to the Navier-Stokes equation with a forcing term  $\mathbf{F}$  linearly proportional to the velocity field  $\mathbf{v}$  [40]. To increase computational efficiency, we employed a discretized version of the ABC flow, the so-called ABC map [31],

$$\begin{aligned} x_{n+1} &= x_n + A \sin z_n + C \cos y_n \text{ mod}(2\pi) \\ y_{n+1} &= y_n + B \sin x_{n+1} + A \cos z_n \text{ mod}(2\pi) \\ z_{n+1} &= z_n + C \sin y_{n+1} + B \cos x_{n+1}, \text{ mod}(2\pi) \end{aligned} \quad (42)$$

to describe the fluid motion in a three dimensional divergence-free flow.

We find that the eigenvectors of the metric tensor of the Lagrangian coordinates converge exponentially in time to their time asymptotic limits in a chaotic region of the flow. In particular, the  $\hat{\mathbf{s}}$  vector converges with an exponent

of  $2\lambda$ , twice the Lyapunov exponent of the flow. Let  $\theta$  and  $\varphi$  be the polar and azimuthal angles of the  $\hat{\mathbf{s}}$  vector in spherical coordinates, one finds that  $d\theta/dt \propto \exp(-2\lambda t)$  and  $d\varphi/dt \propto \exp(-2\lambda t)$ , Fig. 1.

In Fig. 2, we show the probability distribution of  $\lambda(\xi, t = t_0)$  in a single chaotic region. This distribution is approximately Gaussian, but deviations from the Gaussian distribution always occur. The difference between the finite time Lyapunov exponent distribution and a Gaussian distribution becomes smaller as one samples the finite time Lyapunov exponent at a longer time interval (longer  $t_0$ ), Fig. 3. Here the difference is given by *residue* =  $\int \|P(x) - P_n(x, 1, \sigma)\| dx$ , where  $x \equiv \lambda(t)/\lambda^\infty$ ,  $P(x)$  is the distribution function of the finite time Lyapunov exponents and  $P_n(x, 1, \sigma)$  is a normal distribution which is centered at  $x = 1$  and has the same standard deviation  $\sigma$  as that of  $P(x)$ . The standard deviation of the distribution of finite time Lyapunov exponents decreases if the flow is further from being integrable, Fig. 4. For larger  $t_0$  (compared with the Lyapunov time) the standard deviation of the distribution of finite time Lyapunov exponents scales as  $1/\sqrt{t_0}$ , Fig. 5.

We evaluate  $\Delta(\xi, t)$  defined by equation (37) for both the extended standard map and the ABC map, figure 6. It is easy to see that  $\Delta(\xi, t)$  converges exponentially in time, a result that is essential to establish equations (15,16,17), section IV. The strong spatial variation and anisotropy of  $f(\xi, t)$  in equation (15) are illustrated in figure 7. One can see that the correlation length is remarkably long along the  $\hat{\mathbf{s}}$  lines, while it is extremely short in directions away from this orientation. The correlation length of the finite time Lyapunov exponent along the  $\hat{\mathbf{e}}_\infty$  represents the characteristic correlation length in a chaotic flow. The variation of the finite time Lyapunov exponent along an  $\hat{\mathbf{s}}$  line is examined again in figure 8. The geometry of the  $\hat{\mathbf{s}}$  line is represented by the  $\hat{\mathbf{e}}$  and  $\hat{\mathbf{m}}$  components of the  $\hat{\mathbf{s}}$  line curvature. It is easy to see that there is a sharp dip in the magnitude of the finite time Lyapunov exponent wherever the  $\hat{\mathbf{s}}$  line makes a sharp bend. Peculiarly small finite time Lyapunov exponent leads to small local  $\Omega$  number and gives rise to effective diffusion barriers.

## VI. TRANSPORT IN AN INTEGRABLE REGION OF THE FLOW

In an integrable region of a divergence-free flow, neighboring fluid points separate (or converge) at most algebraically. Consequently, the largest eigenvalue  $\Lambda_l$  (or the smallest eigenvalue  $\Lambda_s$ ) of the metric tensor of the Lagrangian coordinates increases (or decreases) at most algebraically. The eigenvectors of the metric tensor still have well-defined time asymptotic limits. Hence the natural Lagrangian coordinates introduced in last section are well-defined in the integrable regions of a flow.

This can be illustrated by considering a divergence-free flow in a bounded integrable region. If there is no null point in the region of interest, a globally divergence-free field admits a Hamiltonian structure [32] to which the machineries in hamiltonian mechanics can be applied. Hence the integrable region of such a divergence-free flow consists of bounded constant ‘‘action’’ surfaces [33], the KAM surfaces. Parameterizing the integrable surfaces using ‘‘action’’ implies the existence of an ‘‘action’’ function  $\Psi(\mathbf{x})$  such that  $\mathbf{v} \cdot \nabla\Psi = 0$  with  $\|\nabla\Psi\| \neq 0$ . Since the flow is also divergence-free ( $\nabla \cdot \mathbf{v} = 0$ ), one can treat it as a one degree of freedom, time dependent Hamiltonian system and write the flow field in the canonical representation, in analogy to the canonical representation of the magnetic field [34]. That is

$$\mathbf{v} = \nabla\Psi \times \nabla\Theta + \nabla\Phi \times \nabla\chi(\Psi) \quad (43)$$

with the hamiltonian  $\chi$  a function of the action-like quantity  $\Psi$  alone. The motion of the fluid element in the  $\Phi$  coordinate is determined by the Jacobian  $J$  of the  $\Psi$ - $\Phi$ - $\Theta$  coordinates,

$$d\Phi/dt = \mathbf{v} \cdot \nabla\Phi = (\nabla\Psi \times \nabla\Theta) \cdot \nabla\Phi = \nu(\Psi, \Phi, \Theta) = 1/J, \quad (44)$$

The Jacobian  $J$  is in general a function of all three coordinates. The angle-like variables  $\Theta$  and time-like variable  $\Phi$  are periodic and we set the period to be  $2\pi$ . The topology of the flow trajectory on a KAM surface is simple in canonical coordinates, and it is given by  $\Theta = \Theta_0 + \iota(\Psi)\Phi$  with  $\iota = d\chi(\Psi)/d\Psi$  the winding number of the flow trajectory. By good KAM surfaces, we mean the surfaces that have irrational winding numbers. Surfaces with a rational winding number consist of closed lines. But a similar line can not close on itself on a good KAM surface.

Straightforward substitution shows that the transformation of  $\Phi = \varphi + \varrho$ ,  $\Theta = \vartheta + \iota\varrho$ , gives the same flow field  $\mathbf{v}$  in canonical form, Eq. (43). Except for the arbitrary function  $\varrho$ , the  $\Psi$ - $\Phi$ - $\Theta$  coordinates are uniquely defined. This limited arbitrariness, in return, allows one to make a transformation of  $\Phi \rightarrow \varphi$  and  $\Theta \rightarrow \vartheta$ , such that the motion of the fluid element on a good KAM surface is prescribed by

$$\Psi = \Psi_0; \quad \varphi = \varphi_0 + \nu_0(\Psi)t; \quad \vartheta = \vartheta_0 + \iota(\Psi)\nu_0(\Psi)t. \quad (45)$$

To prove the existence of equation (45), we need to show that there exists a function  $\varrho(\Psi, \Phi, \Theta)$  such that the Jacobian of the new coordinates  $\Psi$ - $\varphi$ - $\vartheta$  is a function of  $\Psi$  alone, *i.e.*,  $(\nabla\Psi \times \nabla\vartheta) \cdot \nabla\varphi = \nu_0(\Psi)$ . Expressing the

Jacobian of the  $\Psi$ - $\varphi$ - $\vartheta$  coordinates in terms of the new Jacobian (function of  $\Psi$  only) of the transformed coordinates and the transformation function  $\varrho$ , one has

$$\frac{\partial \varrho}{\partial \varphi} + \iota \frac{\partial \varrho}{\partial \vartheta} = \frac{\nu(\Psi, \varphi, \vartheta) - \nu_0}{\nu_0}. \quad (46)$$

The double periodicity in  $\varphi$  and  $\vartheta$  implies that a scalar function  $\nu$  can be written as

$$\nu = \sum_{nm} \nu_{nm} \exp[i(n\varphi - m\vartheta)], \quad (47)$$

and the transformation function  $\varrho$  can be written as

$$\varrho = \sum_{nm} \varrho_{nm} \exp[i(n\varphi - m\vartheta)]. \quad (48)$$

It is easy to show that the Fourier components of the transformation function  $\varrho$  are  $\varrho_{nm} = i\nu_{nm}/(n - m)\nu_0$ . The desired Jacobian of the new coordinates  $\Psi$ - $\varphi$ - $\vartheta$ ,  $1/\nu_0(\Psi)$ , is the  $m = 0$ ,  $n = 0$  Fourier component of  $\nu(\Psi, \varphi, \vartheta)$ , *i.e.*,  $\nu_0(\Psi) = \nu_{00}$ . This proves the existence of  $\Psi$ ,  $\varphi$ ,  $\vartheta$  coordinates in which the motion of fluid element on a good KAM surface satisfies equation (45).

If the system is perturbed away from complete integrability, there exist remnant KAM surfaces which are parameterized on a discontinuous set of action. The trajectory on a KAM surface still follows equation (45) but the action coordinate is generally on a Cantor set. Pöschel showed that on this Cantor set, the KAM surfaces form a differentiable family in the sense of Whitney so one can speak of an integrable system on a Cantor set [35]. The construction of the metric tensor needs the  $\Psi$  derivative of the Jacobian  $\nu_0$  and the rotational transform  $\iota$ . By following Pöschel, the  $\Psi_0$  derivative of  $\nu_0$  and  $\iota$  can be properly defined (in the sense of Whitney) on the remnant KAM surfaces. Except for this subtlety, the results presented in the next two paragraphs on the properties of the metric tensor applies to the remnant KAM surfaces in a perturbed system.

In  $\Psi$ - $\varphi$ - $\vartheta$  coordinates, the Jacobi matrix of the Lagrangian coordinates  $\Psi_0$ - $\varphi_0$ - $\vartheta_0$  is simple,

$$\overleftrightarrow{\mathbf{J}} = \begin{pmatrix} 1 & 0 & 0 \\ \mathcal{A}t & 1 & 0 \\ \mathcal{B}t & 0 & 1 \end{pmatrix}$$

with  $\mathcal{A} = \partial\nu_0/\partial\Psi$  and  $\mathcal{B} = \partial(\iota\nu_0)/\partial\Psi$ . Without losing generality, we write the metric tensor of the  $\Psi$ - $\varphi$ - $\vartheta$  coordinates as

$$\overleftrightarrow{\mathbf{g}}_0 = \begin{pmatrix} \mathcal{C} & \mathcal{D} & \mathcal{E} \\ \mathcal{D} & \mathcal{F} & \mathcal{G} \\ \mathcal{E} & \mathcal{G} & \mathcal{H} \end{pmatrix}$$

where  $\mathcal{C}, \mathcal{D}, \mathcal{E}, \mathcal{F}, \mathcal{G}$  and  $\mathcal{H}$  are the covariant components  $g_{ij}$  of the metric tensor  $\overleftrightarrow{\mathbf{g}}_0$ . The determinant of  $\overleftrightarrow{\mathbf{g}}_0$  in covariant representation is

$$\|\overleftrightarrow{\mathbf{g}}_0\| \equiv J_0^2 \equiv \mathcal{C}\mathcal{F}\mathcal{H} + 2\mathcal{D}\mathcal{E}\mathcal{G} - \mathcal{F}\mathcal{E}^2 - \mathcal{C}\mathcal{G}^2 - \mathcal{H}\mathcal{D}^2. \quad (49)$$

The metric tensor of the Lagrangian coordinates  $\Psi_0$ - $\varphi_0$ - $\vartheta_0$  is given by

$$\overleftrightarrow{\mathbf{g}} = \overleftrightarrow{\mathbf{J}}^T \cdot \overleftrightarrow{\mathbf{g}}_0 \cdot \overleftrightarrow{\mathbf{J}} \quad (50)$$

with  $\overleftrightarrow{\mathbf{J}}^T$  the transpose of  $\overleftrightarrow{\mathbf{J}}$ .

For large  $t$ , the three eigenvalues of the metric tensor ( $\overleftrightarrow{\mathbf{g}}$ ) of the Lagrangian coordinates  $\Psi_0$ - $\varphi_0$ - $\vartheta_0$  are given by

$$\begin{aligned} \Lambda_l &= (\mathcal{F}\mathcal{A}^2 + \mathcal{H}\mathcal{B}^2 + 2\mathcal{G}\mathcal{A}\mathcal{B})t^2 + 2(\mathcal{D}\mathcal{A} + \mathcal{E}\mathcal{B})t + \mathcal{O}(1) \\ \Lambda_m &= \frac{\mathcal{H}\mathcal{F}\mathcal{A}^2 + \mathcal{F}\mathcal{H}\mathcal{B}^2 - \mathcal{G}^2\mathcal{B}^2 - \mathcal{G}^2\mathcal{A}^2}{\mathcal{F}\mathcal{A}^2 + \mathcal{H}\mathcal{B}^2 + 2\mathcal{G}\mathcal{A}\mathcal{B}} + \mathcal{O}(t^{-1}) \\ \Lambda_s &= \frac{J_0^2}{\mathcal{H}\mathcal{F}\mathcal{A}^2 + \mathcal{F}\mathcal{H}\mathcal{B}^2 - \mathcal{G}^2\mathcal{B}^2 - \mathcal{G}^2\mathcal{A}^2} \frac{1}{t^2} + \mathcal{O}(t^{-3}). \end{aligned} \quad (51)$$

The three eigenvectors converge linearly in time to their asymptotic limits,  $\hat{\mathbf{e}}_\infty = (1, 0, 0)$ ,  $\hat{\mathbf{m}}_\infty \propto (0, \iota'\nu_0 + \omega'_0, -\nu'_0)$ ,  $\hat{\mathbf{s}}_\infty \propto (0, \nu'_0, \iota'\nu_0 + \omega'_0)$ , see appendix F. Here the prime denotes a derivative with respect to  $\Psi$ . The

$\hat{\mathbf{e}}$  line is perpendicular to the good KAM surfaces while the  $\hat{\mathbf{s}}$  line and  $\hat{\mathbf{m}}$  line always lie on a good KAM surface. One  $\hat{\mathbf{s}}$  line or one  $\hat{\mathbf{m}}$  line generically fills the whole surface, as they do in a single chaotic region.

If  $\nu_0$  in equation (45) is a constant, the flow is effectively two dimensional. The corresponding  $\hat{\mathbf{e}}$  and  $\hat{\mathbf{s}}$  lines coincide with the action-like variable and the angle-like variable axes. This zero shear case is equivalent to the two dimensional twist map (standard map at  $k=0$ ).

The diffusion coefficients defined in Eqs. (30,31) can be found exactly,

$$D_{ee} = c_0 D; \quad (52)$$

$$D_{em} = c_1 D; \quad (53)$$

$$D_{es} = -c_0 D \varpi t + c_2 D; \quad (54)$$

$$D_{mm} = c_3 D; \quad (55)$$

$$D_{ms} = -c_1 D \varpi t + c_4 D; \quad (56)$$

$$D_{ss} = c_0 D \varpi^2 t^2 - c_2 D \varpi t + c_5 D, \quad (57)$$

where  $c_i$ ,  $i = 0, 5$  are time independent functions of  $\mathcal{A}, \mathcal{B}, \mathcal{C}, \mathcal{D}, \mathcal{E}, \mathcal{F}, \mathcal{G}, \mathcal{H}$ , and their explicit forms are given in appendix G. The shearing rate of the flow is  $\varpi \equiv \sqrt{\mathcal{A}^2 + \mathcal{B}^2}$ . The shearing time  $1/\varpi$  is the characteristic time of a nontrivial integrable flow.

For  $t$  large compared with the shearing time  $1/\varpi$ , the tensor diffusivity is highly anisotropic,  $D_{ee} \approx D_{mm} \approx D_{em} \approx D \ll \|D_{es}\| \approx \|D_{ms}\| \approx D \varpi t \ll D_{ss} \approx D \varpi^2 t^2$ . Hence there are fast diffusion and slow diffusion directions in an integrable flow with shear ( $\nu$  or  $\iota$  is a function of  $\Psi$  instead of a constant). The effective diffusivity in  $\hat{\mathbf{s}}_\infty$  direction increases quadratically in time, so there is a fast diffusion along the  $\hat{\mathbf{s}}_\infty$  lines, which lie on the KAM surface. The  $\hat{\mathbf{e}}_\infty$  vector is perpendicular to the KAM surfaces and the effective diffusivity in  $\hat{\mathbf{e}}_\infty$  direction is the classical diffusivity  $D$ . Hence the diffusion across the KAM surfaces is slow. The natural Lagrangian coordinates defined by equation (18), separate these different diffusion time scales and give the general properties of the passive scalar transport in a generic integrable flow. Since  $\|D_{es}\| \approx D \varpi t$  and the diffusive flux across KAM surfaces has the form of equation (21), there is a period of enhanced diffusive flux across the KAM surfaces during the time in which the fast diffusion is accomplished on the KAM surfaces.

These transport properties can also be demonstrated by solving the diffusion equation (7) with the rough approximations that  $\mathcal{C} = \mathcal{F} = \mathcal{H} = 1$  and  $\mathcal{D} = \mathcal{E} = \mathcal{G} = 0$ . The metric tensor in its contravariant component ( $g^{ij}$ ), now takes the form

$$\vec{\mathbf{g}} = \begin{pmatrix} 1 & -\mathcal{A}t & -\mathcal{B}t \\ -\mathcal{A}t & 1 + \mathcal{A}^2 t^2 & \mathcal{A}\mathcal{B}t^2 \\ -\mathcal{B}t & \mathcal{A}\mathcal{B}t^2 & 1 + \mathcal{B}^2 t^2 \end{pmatrix}$$

For constant  $\mathcal{A}$  and  $\mathcal{B}$ , the diffusion equation can be written as

$$\begin{aligned} \frac{\partial \phi}{\partial t} = & D \frac{\partial^2 \phi}{\partial \Psi_0^2} - 2D\mathcal{A}t \frac{\partial^2 \phi}{\partial \Psi_0 \partial \varphi_0} - 2D\mathcal{B}t \frac{\partial^2 \phi}{\partial \Psi_0 \partial \vartheta_0} + 2D\mathcal{A}\mathcal{B}t^2 \frac{\partial^2 \phi}{\partial \varphi_0 \partial \vartheta_0} \\ & + D(1 + \mathcal{A}^2 t^2) \frac{\partial^2 \phi}{\partial \varphi_0^2} + D(1 + \mathcal{B}^2 t^2) \frac{\partial^2 \phi}{\partial \vartheta_0^2}. \end{aligned} \quad (58)$$

The general solution to this equation is

$$\phi(\Psi_0, \varphi_0, \vartheta_0, t) = (2\pi)^{-3/2} \iiint_{-\infty}^{\infty} \tilde{\phi}(k_\Psi, k_\varphi, k_\vartheta, t) e^{i(k_\Psi \Psi_0 + k_\varphi \varphi_0 + k_\vartheta \vartheta_0)} dk_\Psi dk_\varphi dk_\vartheta \quad (59)$$

where

$$\tilde{\phi}(k_\Psi, k_\varphi, k_\vartheta, t) = \tilde{\phi}_0(k_\Psi, k_\varphi, k_\vartheta) e^{-Dk_\Psi^2 t + \mathcal{A}t^2 Dk_\Psi k_\varphi + \mathcal{B}t^2 Dk_\Psi k_\vartheta - (2\mathcal{A}\mathcal{B}t^3/3) Dk_\varphi k_\vartheta - (t + \mathcal{A}^2 t^3/3) Dk_\varphi^2 - (t + \mathcal{B}^2 t^3/3) Dk_\vartheta^2} \quad (60)$$

$$= \tilde{\phi}_0(k_\Psi, k_\varphi, k_\vartheta) e^{-Dt[k_\Psi^2 + k_\varphi^2 + k_\vartheta^2 - \mathcal{A}t k_\Psi k_\varphi - \mathcal{B}t k_\Psi k_\vartheta + (\mathcal{A}t k_\varphi + \mathcal{B}t k_\vartheta)^2/3]} \quad (61)$$

with  $\tilde{\phi}_0(k_\Psi, k_\varphi, k_\vartheta)$  given by the initial condition  $\phi_0 \equiv \phi(\Psi_0, \varphi_0, \vartheta_0, t = 0)$

$$\begin{aligned} \tilde{\phi}_0(k_\Psi, k_\varphi, k_\vartheta) & \equiv \tilde{\phi}(k_\Psi, k_\varphi, k_\vartheta, t = 0) \\ & = (2\pi)^{-3/2} \iiint_{-\infty}^{\infty} \phi_0(\Psi_0, \varphi_0, \vartheta_0) e^{i(k_\Psi \Psi_0 + k_\varphi \varphi_0 + k_\vartheta \vartheta_0)} d\Psi_0 d\varphi_0 d\vartheta_0. \end{aligned} \quad (62)$$

Let  $\tau_{\parallel}$  and  $\tau_{\perp}$  be the characteristic diffusion times of the initial passive scalar field in and across the KAM surfaces. The characteristic dimensionless quantity is the ratio between the characteristic diffusion time and the shearing time of the flow,  $\Omega \equiv \varpi\tau_{\parallel}$ . For  $\Omega \gg 1$ , the scalar field is advected by the flow until time  $t_a \equiv \Omega^{1/3}/\varpi$ , which is much shorter than the characteristic diffusion time of the initial scalar field. In the KAM surface, the spatial dependence ( $\varphi_0$  and  $\vartheta_0$ ) of the passive scalar field  $\phi$  is damped after another  $t_a$ , *i.e.*,  $\partial\phi/\partial\varphi_0 \approx \partial\phi/\partial\vartheta_0 \approx 0$  for  $t > 2t_a$ . The asymptotic form for the passive scalar field  $\phi$  is determined by the slow varying  $\Psi_0$  dependence, *i.e.*, for  $t > 2t_a$ ,

$$\phi(\Psi_0, t) = (2\pi)^{-1/2} \int_{-\infty}^{\infty} \tilde{\phi}_0(k_{\Psi}, 0, 0) e^{ik_{\Psi}\Psi_0 - Dk_{\Psi}^2 t} dk_{\Psi}, \quad (63)$$

with

$$\tilde{\phi}_0(k_{\Psi}, 0, 0) = (2\pi)^{-3/2} \iiint_{-\infty}^{\infty} \phi_0(\Psi_0, \varphi_0, \vartheta_0) e^{ik_{\Psi}\Psi_0} d\Psi_0 d\varphi_0 d\vartheta_0, \quad (64)$$

and  $\phi_0(\Psi_0, \varphi_0, \vartheta_0)$  the initial field. Hence the smoothing of the gradient of  $\phi$  across the KAM surfaces has a long tail and is accurately described by the characteristic diffusion time  $\tau_{\perp}$ ,  $\partial\phi/\partial\Psi_0 \propto \exp(-t/\tau_{\perp})$ .

In summary, the fast diffusion which is the result of shearing between different KAM surfaces and the constraint of the flow being divergence-free, occurs only within the KAM surfaces. Diffusion across the KAM surfaces is approximated by the characteristic diffusion time and is very slow. In the case of the temperature of electrons confined on good magnetic surfaces in fusion devices, the electron temperature quickly relaxes to thermal equilibrium on the good magnetic surfaces, while the heat transfer across magnetic surfaces is much slower and described by a cross-field thermal diffusion time. On the contrary, electron temperature variations are rapidly damped in the region of stochastic field lines, since an  $\hat{s}$  line in which there is a rapid diffusion, generically fills the whole region explored by the stochastic field line.

## VII. SUMMARY

The advection and diffusion of a passive scalar have been investigated in both chaotic and integrable flows. The characteristic time scale of a chaotic flow is the Lyapunov time which measures the exponential convergence of neighboring fluid elements. The characteristic dimensionless quantity for the chaotic transport problem is the ratio between the characteristic diffusion time of the scalar field and the Lyapunov time of the flow. This number is in general very large. The scalar field is purely advected by the flow until the time  $t_a - 1/2\lambda$  with  $t_a \equiv \ln 2\Omega/2\lambda$ . There is a rapid diffusion during a relatively short interval ( $1/\lambda$ ) centered on time  $t_a$ . This rapid diffusion occurs only along the field line of the  $\hat{s}_{\infty}$ , which defines the stable direction for the streamlines. The fast diffusion can be confined to one coordinate in natural Lagrangian coordinates. The rapid diffusion removes the gradient of the scalar field in the entire chaotic region.

The finite time Lyapunov exponent varies smoothly along an  $\hat{s}$  line and has sharp dips where the  $\hat{s}$  line makes a sharp bend. A large reduction in  $\lambda$  leads to a peculiarly small  $\Omega$  number. Hence the sharp bends of the  $\hat{s}$  line define a class of barriers for diffusion. This new class of diffusion barriers are associated with the non-hyperbolicity of the system, which is thought to be generic for chaotic systems [2].

The characteristic time scale of an integrable flow with shear is the time scale on which neighboring fluid points separate algebraically due to the shear. The characteristic dimensionless quantity for the transport of a passive scalar in such flow is the ratio between the characteristic diffusion time of the scalar field and the shearing time of the flow,  $\Omega \equiv \tau_d\varpi$ . If the shearing time of the flow is much faster than the characteristic diffusion time, the scalar field is advected by the flow until time  $t_a \equiv \Omega^{1/3}/\varpi$ . The fast diffusion, which is confined within the KAM surfaces, removes the gradient of the scalar field in the KAM surfaces after time interval  $t_a$ . During the period ( $t_a < t < 2t_a$ ), there is an enhanced diffusive flux (compared with the one predicted by the characteristic diffusion time) across the KAM surfaces, but it is too small to remove the  $\Psi_0$  dependence. For  $t > 2t_a$ , the scalar field has only  $\Psi$  dependence, and its decay is accurately described by the characteristic diffusion time. Hence, across the KAM surfaces, the diffusion is distinctly slow and a large gradient of the scalar field can be maintained.

## ACKNOWLEDGMENTS

We would like to thank U. S. Department of Energy for support under grant DE-FG02-97ER54441. Part of the research was done while one of the authors (Tang) was supported by a NSF University-Industry Postdoctoral Fellowship in Mathematical Sciences through SUNY Stony Brook.

## APPENDIX A: CHAOTIC FLOW AND THE ERGODIC THEOREM OF DYNAMICAL SYSTEMS

If a flow field is smooth, the equation of motion for the fluid element, Eq. (4), can be treated as a differentiable dynamical system to which the ergodic theorem of dynamical systems [3] can be applied.

For simplicity, we consider a steady flow,  $d\mathbf{x}/dt = \mathbf{v}(\mathbf{x})$ ,  $\mathbf{x} \in \mathfrak{R}^3$ , or a time-periodic flow which can be reduced to a map,  $\mathbf{x}_{n+1} = \mathbf{V}(\mathbf{x}_n)$ ,  $\mathbf{x}_n \in \mathfrak{R}^3$ . We also assume that the flow is time reversible. The distance between neighboring points at time  $t$  is related to their initial separation by  $dl^2 = g_{ij}d\xi^i d\xi^j$ , with  $g_{ij}$  the metric tensor of the Lagrangian coordinates. The rate of the exponential divergence or convergence of neighboring trajectories is measured by the Lyapunov exponent,  $\lambda = \lim_{t \rightarrow \infty} (1/2t) \ln(dl^2/dl_0^2)$ . In vector form,

$$\lambda(\xi, \mathbf{u}) = \lim_{t \rightarrow \infty} \ln(\mathbf{u} \cdot \overleftrightarrow{\mathbf{g}} \cdot \mathbf{u})/2t. \quad (\text{A1})$$

Here  $\mathbf{u}$  specifies the direction along which the initial fluid points separate, *i.e.*,  $\overline{\delta_0} = \delta_0 \mathbf{u}$ .

In a single chaotic region (the region in which an ergodic measure is preserved by the time evolution of the fluid equation), the multiplicative ergodic theorem asserts that there exist three characteristic directions in which three Lyapunov exponents reside, *i.e.*,

$$\lambda_i = \lambda(\xi, \hat{\mathbf{e}}^i) = \lim_{t \rightarrow \infty} \ln(\hat{\mathbf{e}}^i \cdot \overleftrightarrow{\mathbf{g}} \cdot \hat{\mathbf{e}}^i)/2t, \quad i = 1, 2, 3. \quad (\text{A2})$$

The Lyapunov exponents are independent of position  $\xi$  in a single chaotic region. If there is no degeneracy in Lyapunov exponents,  $\lambda_1 > \lambda_2 > \lambda_3$ , which is trivially true for a chaotic divergence-free flow, the three-dimensional basis  $\hat{\mathbf{e}}^i$ ,  $i = 1, 2, 3$ , which are functions of Lagrangian coordinates alone, are distinct and span  $\mathfrak{R}^3$ . For a rigorous mathematical proof, see [20] and [36]. For a general discussion, see [39]. Generically,  $\hat{\mathbf{e}}^i$ ,  $i = 1, 2, 3$ , are not orthogonal to each other. The eigenvectors of the metric tensor of the Lagrangian coordinates are orthogonal to each other, and their time asymptotic limits are uniquely related to the characteristic directions  $\hat{\mathbf{e}}^i$  by

$$\hat{\mathbf{e}}_\infty \propto \hat{\mathbf{e}}^2 \times \hat{\mathbf{e}}^3; \quad \hat{\mathbf{m}}_\infty \propto \hat{\mathbf{e}}^2 - (\hat{\mathbf{e}}^2 \cdot \hat{\mathbf{e}}^3)\hat{\mathbf{e}}^3; \quad \hat{\mathbf{s}}_\infty = \hat{\mathbf{e}}^3. \quad (\text{A3})$$

The finite time eigenvectors converge exponentially to their time asymptotic limit, Fig. 1 in section V.

In an integrable region of the flow, the Lyapunov exponents vanish. But for a nontrivial flow (flow with shear), there exist non-degenerate characteristic directions which are associated with the center unstable, center, and center stable manifolds [37]. Hence the eigenvectors of the metric tensor still have well-defined time asymptotic limits, but with an algebraic convergence rate, as we showed in section VI.

## APPENDIX B: ADVECTION AND DIFFUSION IN A FLOW WITH $\lambda_M^\infty \neq 0$

The approach presented in this paper can be applied to flows with an arbitrary combination of positive and negative Lyapunov exponents. The trajectory of a flow point, which is the solution to equation  $d\mathbf{x}/dt = \mathbf{v}(\mathbf{x}, t)$ , is characterized by at most three Lyapunov exponents. For a general time-dependent divergence-free flow, there are always one positive ( $\lambda_l > 0$ ) and one negative ( $\lambda_s < 0$ ). The middle one  $\lambda_m$  might be non-zero. If  $\lambda_m > 0$ , the effective diffusivity in  $\hat{\mathbf{m}}_\infty$  direction

$$D_{mm} \equiv \hat{\mathbf{m}}_\infty \cdot \overleftrightarrow{\mathbf{D}} \cdot \hat{\mathbf{m}}_\infty \approx D / \exp(2\lambda_m t)$$

decreases exponentially in time, just like that in the  $\hat{\mathbf{e}}_\infty$  direction. Consequently, diffusion occurs only along the field line of the  $\hat{\mathbf{s}}_\infty$  vector.

Even if  $\lambda_m < 0$ , the rapid diffusion in a chaotic flow occurs only along the  $\hat{\mathbf{s}}$  line, as long as  $\lambda_m$  does not have a value very close to that of  $\lambda_s$ . This can be seen by comparing the effective diffusivities in  $\hat{\mathbf{m}}_\infty$  and  $\hat{\mathbf{s}}_\infty$  directions at time  $t_a \equiv \ln(2\Omega)/2|\lambda_s|$  with  $\Omega \equiv |\lambda_s|L^2/D$ ,

$$\frac{D_{mm}}{D_{ss}} \approx \exp[2(|\lambda_m| - |\lambda_s|)t_a] = (2\Omega)^{-1+|\lambda_m|/|\lambda_s|}.$$

For  $\Omega \gg 1$  which is the case for most practical problems,  $D_{mm}/D_{ss} \ll 1$  if  $\lambda_m \neq \lambda_s$ . That is, the diffusion occurs only along the  $\hat{\mathbf{s}}$  line. If  $\lambda_m = \lambda_s$ , diffusion occurs in the  $(\hat{\mathbf{m}}_\infty, \hat{\mathbf{s}}_\infty)$  surfaces and diffusion barriers appear where both  $\lambda_m$  and  $\lambda_s$  have peculiarly small values.



## APPENDIX C: CONSTRUCTION OF NATURAL LAGRANGIAN COORDINATES

If  $\hat{\mathbf{s}}_\infty$  is an arbitrary vector field, one can find a function  $g(\xi)$  such that  $e^{-g(\xi)}\hat{\mathbf{s}}_\infty$  is divergence free, for  $\nabla \cdot (e^{-g(\xi)}\hat{\mathbf{s}}_\infty) = (-\hat{\mathbf{s}}_\infty \cdot \nabla g(\xi) + \nabla \cdot \hat{\mathbf{s}}_\infty)e^{-g(\xi)}$  can be made to vanish by solving for  $g(\xi)$  such that  $\hat{\mathbf{s}}_\infty \cdot \nabla g = \nabla \cdot \hat{\mathbf{s}}_\infty$ . Divergence-free fields can be represented in Euler potentials [38]  $\alpha$  and  $\zeta$ , *i.e.*,  $e^{-g(\xi)}\hat{\mathbf{s}}_\infty = \nabla\zeta \times \nabla\alpha$ . Hence an arbitrary field  $\hat{\mathbf{s}}_\infty$  can be written in the Clebsch representation,

$$\hat{\mathbf{s}}_\infty = e^{g(\xi)}\nabla\zeta \times \nabla\alpha \quad (\text{C1})$$

where the Euler potentials  $\alpha(\xi)$  and  $\zeta(\xi)$  are locally defined functions such that  $\hat{\mathbf{s}}_\infty \cdot \nabla\alpha = 0$  and  $\hat{\mathbf{s}}_\infty \cdot \nabla\zeta = 0$ .

Using the dual relations [32], we can relate the third coordinate  $\beta$  to the  $\hat{\mathbf{s}}_\infty$  field, *i.e.*,

$$\hat{\mathbf{s}}_\infty = \frac{e^{g(\xi)}}{J} \frac{\partial \xi}{\partial \beta} \quad (\text{C2})$$

with  $J = 1/(\nabla\alpha \times \nabla\beta) \cdot \nabla\zeta$  the Jacobian of the  $\alpha$ - $\beta$ - $\zeta$  coordinates. The choice of the Jacobian is free. One can let  $J = 1$  or  $J = e^{g(\xi)}$ .

Since  $\hat{\mathbf{e}}_\infty = \hat{\mathbf{m}}_\infty \times \hat{\mathbf{s}}_\infty$  and  $\hat{\mathbf{m}}_\infty = \hat{\mathbf{s}}_\infty \times \hat{\mathbf{e}}_\infty$ , one can show

$$\hat{\mathbf{e}}_\infty = -(\hat{\mathbf{m}}_\infty \cdot \nabla\zeta)e^{g(\xi)}\nabla\alpha + (\hat{\mathbf{m}}_\infty \cdot \nabla\alpha)e^{g(\xi)}\nabla\zeta \quad (\text{C3})$$

$$\hat{\mathbf{m}}_\infty = (\hat{\mathbf{e}}_\infty \cdot \nabla\zeta)e^{g(\xi)}\nabla\alpha - (\hat{\mathbf{e}}_\infty \cdot \nabla\alpha)e^{g(\xi)}\nabla\zeta. \quad (\text{C4})$$

The  $\hat{\mathbf{s}}_\infty$  vector can be written in the general covariant form,

$$\hat{\mathbf{s}}_\infty = a_1\nabla\alpha + a_2\nabla\beta + a_3\nabla\zeta, \quad (\text{C5})$$

where only  $a_2$  is constrained by  $a_2 = J/e^{g(\xi)}$ . Equations (C3)-(C5) have the required form to yield equation (18) of the paper. It is interesting to note that one choice of  $g(\xi)$  is  $\lambda$  in equation (15).

## APPENDIX D: THE EIGENVECTORS OF THE METRIC TENSOR

For a general three dimensional flow, one has

$$g_{ij} = \Lambda_l e_i e_j + \Lambda_m m_i m_j + \Lambda_s s_i s_j \quad (\text{D1})$$

and

$$g^{ij} = E^i E^j / \Lambda_l + M^i M^j / \Lambda_m + S^i S^j / \Lambda_s \quad (\text{D2})$$

with the eigenvalues  $\Lambda_l \geq \Lambda_m \geq \Lambda_s > 0$ . Here  $e_i, m_i, s_i$  are the covariant components of the vectors  $\hat{\mathbf{e}}, \hat{\mathbf{m}}, \hat{\mathbf{s}}$ , while  $E^i, M^i, S^i$  are the contravariant components of the vectors  $\hat{\mathbf{E}}, \hat{\mathbf{M}}, \hat{\mathbf{S}}$ . They satisfy the relations:  $e_i e_j + m_i m_j + s_i s_j = \delta_{ij}$ ;  $E^i E^j + M^i M^j + S^i S^j = \delta^{ij}$ ;  $\sum e_i E^i = \sum m_i M^i = \sum s_i S^i = 1$ ;  $\sum e_i M^i = \sum e_i S^i = \sum m_i E^i = \sum m_i S^i = \sum s_i E^i = \sum s_i M^i = 0$ . In vector form, that is:  $\hat{\mathbf{e}} \cdot \hat{\mathbf{E}} = \hat{\mathbf{m}} \cdot \hat{\mathbf{M}} = \hat{\mathbf{s}} \cdot \hat{\mathbf{S}} = 1$  and  $\hat{\mathbf{e}} \cdot \hat{\mathbf{M}} = \hat{\mathbf{e}} \cdot \hat{\mathbf{S}} = \hat{\mathbf{m}} \cdot \hat{\mathbf{E}} = \hat{\mathbf{m}} \cdot \hat{\mathbf{S}} = \hat{\mathbf{s}} \cdot \hat{\mathbf{E}} = \hat{\mathbf{s}} \cdot \hat{\mathbf{M}} = 0$ .

To find the dot product of two vectors both of which are in the same form (covariant or contravariant), one has to specify the metric tensor. In real space, the metric tensor of the Lagrangian coordinates is given in equations (D1,D2), hence one has  $\hat{\mathbf{e}} \cdot \hat{\mathbf{e}} = \sum e_i g^{ij} e_j = 1/\Lambda_l$ ,  $\hat{\mathbf{m}} \cdot \hat{\mathbf{m}} = \sum m_i g^{ij} m_j = 1/\Lambda_m$ ,  $\hat{\mathbf{s}} \cdot \hat{\mathbf{s}} = \sum s_i g^{ij} s_j = 1/\Lambda_s$ ,  $\hat{\mathbf{E}} \cdot \hat{\mathbf{E}} = \sum E^i g_{ij} E^j = \Lambda_l$ ,  $\hat{\mathbf{M}} \cdot \hat{\mathbf{M}} = \sum M^i g_{ij} M^j = \Lambda_m$ ,  $\hat{\mathbf{S}} \cdot \hat{\mathbf{S}} = \sum S^i g_{ij} S^j = \Lambda_s$ .

In Lagrangian space, the metric tensor  $g_0^{ij}$  of the Lagrangian coordinates (which are taken to be Cartesian coordinates) is the unit matrix. Hence  $\hat{\mathbf{e}}(\hat{\mathbf{m}}, \hat{\mathbf{s}})$  can not be distinguished from  $\hat{\mathbf{E}}(\hat{\mathbf{M}}, \hat{\mathbf{S}})$  and one can label them with  $\hat{\mathbf{e}}_0, \hat{\mathbf{m}}_0$  and  $\hat{\mathbf{s}}_0$  for clarity. It is easy to see that  $\hat{\mathbf{e}}_0 \cdot \hat{\mathbf{e}}_0 = \sum e_i g_0^{ij} e_j = 1$ ,  $\hat{\mathbf{m}}_0 \cdot \hat{\mathbf{m}}_0 = \sum m_i g_0^{ij} m_j = 1$ , and  $\hat{\mathbf{e}}_0 \cdot \hat{\mathbf{m}}_0 = \hat{\mathbf{e}}_0 \cdot \hat{\mathbf{s}}_0 = \hat{\mathbf{m}}_0 \cdot \hat{\mathbf{s}}_0 = 0$ . Most discussions in the paper are within Lagrangian space, so we drop the subscript for simplicity. Hence  $\hat{\mathbf{s}}$  in the main body of the paper should be understood as  $\hat{\mathbf{s}}_0$  and  $\hat{\mathbf{s}}_\infty$  is the time asymptotic limit of  $\hat{\mathbf{s}}_0$ .

## APPENDIX E: THE DERIVATIVES OF THE METRIC TENSOR

The spatial derivative of the metric tensor in Lagrangian coordinates is

$$\begin{aligned} \frac{\partial g_{ij}}{\partial \xi^k} &= \frac{\partial \Lambda_l}{\partial \xi^k} e_i e_j + \Lambda_l \frac{\partial e_i}{\partial \xi^k} e_j + \Lambda_l e_i \frac{\partial e_j}{\partial \xi^k} \\ &+ \frac{\partial \Lambda_m}{\partial \xi^k} m_i m_j + \Lambda_m \frac{\partial m_i}{\partial \xi^k} m_j + \Lambda_m m_i \frac{\partial m_j}{\partial \xi^k} \\ &+ \frac{\partial \Lambda_s}{\partial \xi^k} s_i s_j + \Lambda_s \frac{\partial s_i}{\partial \xi^k} s_j + \Lambda_s s_i \frac{\partial s_j}{\partial \xi^k}. \end{aligned} \quad (\text{E1})$$

Using the various orthonormal relationships outlined in appendix D, one finds

$$\hat{\mathbf{S}} \cdot \frac{\partial \vec{\mathbf{g}}}{\partial \xi^k} \cdot \hat{\mathbf{S}} = \frac{\partial \Lambda_s}{\partial \xi^k}; \quad (\text{E2})$$

$$\hat{\mathbf{E}} \cdot \frac{\partial \vec{\mathbf{g}}}{\partial \xi^k} \cdot \hat{\mathbf{S}} = (\Lambda_l - \Lambda_s) \hat{\mathbf{e}}_0 \cdot \frac{\partial \hat{\mathbf{s}}_0}{\partial \xi^k}; \quad (\text{E3})$$

$$\hat{\mathbf{M}} \cdot \frac{\partial \vec{\mathbf{g}}}{\partial \xi^k} \cdot \hat{\mathbf{S}} = (\Lambda_m - \Lambda_s) \hat{\mathbf{m}}_0 \cdot \frac{\partial \hat{\mathbf{s}}_0}{\partial \xi^k}, \quad (\text{E4})$$

where  $\hat{\mathbf{e}}_0$ ,  $\hat{\mathbf{m}}_0$ , and  $\hat{\mathbf{s}}_0$  are orthonormal vectors in Lagrangian space, appendix D. The spatial derivative of vector  $\hat{\mathbf{s}}_0$  is given by

$$\frac{\partial \hat{\mathbf{s}}_0}{\partial \xi^k} = [\hat{\mathbf{E}} \cdot \frac{\partial \vec{\mathbf{g}}}{\partial \xi^k} \cdot \hat{\mathbf{S}} / (\Lambda_l - \Lambda_s)] \hat{\mathbf{e}}_0 + [\hat{\mathbf{M}} \cdot \frac{\partial \vec{\mathbf{g}}}{\partial \xi^k} \cdot \hat{\mathbf{S}} / (\Lambda_m - \Lambda_s)] \hat{\mathbf{m}}_0. \quad (\text{E5})$$

The divergence of  $\hat{\mathbf{s}}_0$  vector can be found from the various component of this equation. Since  $\Lambda_s = \exp(2\lambda_s t) = \exp(-2\lambda t)$ , the spatial derivative of the finite time Lyapunov exponent is related to the derivatives of the metric tensor by

$$\frac{\partial \lambda t}{\partial \xi^k} = -\frac{1}{2\Lambda_s} \left( \hat{\mathbf{S}} \cdot \frac{\partial \vec{\mathbf{g}}}{\partial \xi^k} \cdot \hat{\mathbf{S}} \right) \quad (\text{E6})$$

Hence  $\hat{\mathbf{s}}_0 \cdot \nabla_0 \lambda t + \nabla_0 \cdot \hat{\mathbf{s}}_0$  can be directly calculated using the spatial derivatives of the metric tensor, which have analytical expressions if the flow field is specified in the form of an explicit function of space and time.

## APPENDIX F: CONVERGENCE OF $\hat{\mathbf{e}}$ , $\hat{\mathbf{m}}$ AND $\hat{\mathbf{s}}$ VECTORS IN AN INTEGRABLE REGION OF THE FLOW

If we write the eigenvectors of the metric tensor  $\vec{\mathbf{g}}$  (Eq. (50)) of the Lagrangian coordinates  $\Psi_0 - \varphi_0 - \vartheta_0$  in their covariant components, *i.e.*,  $\hat{\mathbf{e}} = (e_\Psi, e_\varphi, e_\vartheta)$ ,  $\hat{\mathbf{m}} = (m_\Psi, m_\varphi, m_\vartheta)$  and  $\hat{\mathbf{s}} = (s_\Psi, s_\varphi, s_\vartheta)$ , one finds that in an integrable region of the flow,

$$\frac{e_\Psi}{e_\vartheta} = \frac{\mathcal{F}\mathcal{A}^2 + \mathcal{H}\mathcal{B}^2 + 2\mathcal{G}\mathcal{A}\mathcal{B}}{\mathcal{G}\mathcal{A} + \mathcal{H}\mathcal{B}} t + \frac{2\mathcal{G}\mathcal{D}\mathcal{A}^2 - \mathcal{F}\mathcal{E}\mathcal{A}^2 + \mathcal{H}\mathcal{E}\mathcal{B}^2 + 2\mathcal{D}\mathcal{H}\mathcal{A}\mathcal{B}}{(\mathcal{G}\mathcal{A} + \mathcal{H}\mathcal{B})^2} + \mathcal{O}(t^{-1}); \quad (\text{F1})$$

$$\frac{e_\varphi}{e_\vartheta} = \frac{\mathcal{F}\mathcal{A} + \mathcal{G}\mathcal{B}}{\mathcal{G}\mathcal{A} + \mathcal{H}\mathcal{B}} + \mathcal{O}(t^{-1}); \quad (\text{F2})$$

$$\frac{m_\Psi}{m_\vartheta} = \frac{-\mathcal{G}\mathcal{A}^2 - \mathcal{H}\mathcal{A}\mathcal{B} + \mathcal{F}\mathcal{A}\mathcal{B} + \mathcal{G}\mathcal{B}^2}{2\mathcal{G}\mathcal{A}^2\mathcal{B} + \mathcal{H}\mathcal{A}\mathcal{B}^2 + \mathcal{F}\mathcal{A}^3} \frac{1}{t} + \mathcal{O}(t^{-2}); \quad (\text{F3})$$

$$\frac{m_\varphi}{m_\vartheta} = -\frac{\mathcal{B}}{\mathcal{A}} + \mathcal{O}(t^{-1}); \quad (\text{F4})$$

$$\frac{s_\Psi}{s_\vartheta} = -\frac{1}{\mathcal{B}t} + \mathcal{O}(t^{-2}); \quad (\text{F5})$$

$$\frac{s_\varphi}{s_\vartheta} = \frac{\mathcal{A}}{\mathcal{B}} + \mathcal{O}(t^{-1}). \quad (\text{F6})$$

Hence in the integrable region of the flow,  $\hat{\mathbf{e}}$ ,  $\hat{\mathbf{m}}$  and  $\hat{\mathbf{s}}$  vectors converge linearly in time to their time asymptotic limits,  $\hat{\mathbf{e}}_\infty \propto (1, 0, 0)$ ,  $\hat{\mathbf{m}}_\infty \propto (0, \mathcal{B}, -\mathcal{A})$  and  $\hat{\mathbf{s}}_\infty \propto (0, \mathcal{A}, \mathcal{B})$ .

APPENDIX G: DIFFUSIVITY COEFFICIENTS

$$c_0 = (\mathcal{FH} - \mathcal{G}^2)/J_0^2; \tag{G1}$$

$$c_1 = (\mathcal{BHD} - \mathcal{BGE} + \mathcal{AGD} - \mathcal{AFE})/(J_0^2 \sqrt{\mathcal{A}^2 + \mathcal{B}^2}); \tag{G2}$$

$$c_2 = (-\mathcal{AHD} + \mathcal{AGE} + \mathcal{BGD} - \mathcal{BFE})/(J_0^2 \sqrt{\mathcal{A}^2 + \mathcal{B}^2}); \tag{G3}$$

$$c_3 = \frac{\mathcal{B}^2\mathcal{HC} - \mathcal{B}^2\mathcal{E}^2 + 2\mathcal{BAGC} - 2\mathcal{BADE} + \mathcal{A}^2\mathcal{FC} - \mathcal{A}^2\mathcal{D}^2}{J_0^2(\mathcal{A}^2 + \mathcal{B}^2)}; \tag{G4}$$

$$c_4 = \frac{\mathcal{B}^2\mathcal{GC} - \mathcal{A}^2\mathcal{GC} + \mathcal{A}^2\mathcal{DE} - \mathcal{BAHC} - \mathcal{B}^2\mathcal{DE} - \mathcal{ABD}^2 + \mathcal{BAE}^2 + \mathcal{ABFC}}{J_0^2(\mathcal{A}^2 + \mathcal{B}^2)}; \tag{G5}$$

$$c_5 = \frac{\mathcal{B}^2\mathcal{FC} - \mathcal{B}^2\mathcal{D}^2 + \mathcal{A}^2\mathcal{HC} + 2\mathcal{BADE} - 2\mathcal{BAGC} - \mathcal{A}^2\mathcal{E}^2}{J_0^2(\mathcal{A}^2 + \mathcal{B}^2)}; \tag{G6}$$

Here  $J_0^2$  is the determinant of the metric tensor of the  $\Psi$ - $\varphi$ - $\vartheta$  coordinates, Eq. (49).

[1] L. D. Landau and E. M. Lifshitz, *Fluid Mechanics*, (Pegamon Press, Oxford, 1959 ), Chapter vi.

[2] X. Z. Tang and A. H. Boozer, *Physica D* **95** 283 (1996).

[3] J.-P. Eckmann and D. Ruelle, *Rev. Modern Phys.* **57** (1985) 617.

[4] G.I. Taylor, *Proc. R. Soc., A* **20** (1921) 196.

[5] Ya.B. Zeldovich, S.A. Molchanov, A.A. Ruzmaikin, and D.D. Sokoloff, *Sov. Sci. Rev. C. Math. Phys.* Vol. 7, 1988 pp. 1-110.

[6] J.A. Krommes, *Phys. Plasmas* **4** (1997) 1342.

[7] H. Aref, *J. Fluid Mech.*, **143**, 1 (1984); H. Aref, S. W. Jones, and O. M. Thomas, *Comput. Phys.* **2**, 22 (1988).

[8] R.R. Prasad, C. Meneveau, and K.R. Sreenivasan, *Phys. Rev. Lett.* **61**, 74 (1988); J. C. Sommerer and E. Ott, *Science* **259**, 335 (1993).

[9] T. H. Solomon and J. P. Gollub, *Phys. Rev. A* **38**, 6280 (1988); R. P. Behringer, S. D. Meyers, and H. L. Swinney, *Phys. Fluids A* **3**, 1243 (1991); T. H. Solomon, E. R. Weeks, and H. L. Swinney, *Phys. Rev. Lett.* **71**, 3975 (1993).

[10] J.D. Meiss, *Rev. Modern Phys.* **64** (1992) 795.

[11] G.M. Zaslavsky, *Physica D* **76** (1994) 110.

[12] I.C. Percival, "Variational principles for invariant tori and cantori," in *Nonlinear dynamics and beam-beam interaction*, edited by M. Month and J.C. Herrera (AIP, New York, 1979); S. Aubry, "The new concept of transitions by breaking of analyticity in a crystallographic mode," in *Soliton and condensed matter physics*, Springer series in solid state physics, Vol.8, edited by A.R. Bishop and T. Schneider (Springer-Verlag, New York, 1978).

[13] R.S. Mackay, J.D. Meiss, and I.C. Percival, *Physica D* **13** (1984) 55.

[14] J.D. Meiss and E. Ott, *Physica D* **6** (1986) 375.

[15] D. Beigie, A. Leonard, and S. Wiggins, *Chaos, Solitons & Fractals*, Vol. 4 (1994) 749.

[16] Albert Einstein, *Investigations on the theory of the Brownian movement* (Dover, New York, 1956).

[17] A.B. Rechester and M.N. Rosenbluth, *Phys. Rev. Lett.* **40** (1978) 38.

[18] M.N. Rosenbluth, R.Z. Sagdeev, J.B. Taylor, and G.M. Zaslavsky, *Nucl. Fusion* **6** (1966) 297; N.N. Filonenko, R.Z. Sagdeev, and G.M. Zaslavsky, *Nucl. Fusion* **7** (1967) 253.

[19] C.F.F. Karney, A.B. Rechester, and R.B. White, *Physica D* **4** (1982) 425.

[20] V. I. Oseledec, *Moscow Math. Soc.* **19**, 197 (1968).

[21] X.Z. Tang and A.H. Boozer, *Phys. Lett. A* **236** (1997) 476.

[22] E. Ott and T. M. Antonsen, Jr., *Phys. Rev. Lett.* **61**, 2839 (1988), *Phys. Rev. A* **39**, 3660 (1989); T. M. Antonsen, Jr. and E. Ott, *Phys. Rev. A* **44**, 851 (1991).

[23] J. M. Ottino, *Annu. Rev. Fluid Mech.* **22**, 207 (1990); J. M. Ottino, *The Kinematics of Mixing: Stretching, Chaos and Transport* ( Cambridge University Press, Cambridge, 1989); S. Wiggins, *Chaotic Transport in Dynamical System* (Spring-Verlag, New York, 1992).

[24] X. Z. Tang, Ph. D. dissertation, the College of William and Mary in Virginia, 1995.

[25] We note that previous analyses by others [26,27] have employed a Lagrangian approach, but they are only locally valid, in contrast to the global (Lagrangian) coordinate transformation used in [2] and this paper.

[26] J. M. Ottino, *J. Fluid Mech.* **114**, 83 (1982).

- [27] D. Beige, A. Leonard, and S. Wiggins, *Phys. Fluids A* **3**, 1039 (1991).
- [28] G. K. Batchelor, *Fluid Mech.* **5** (1959) 113.
- [29] D. P. Stern, *American Journal of Physics* **38**, 494 (1970).
- [30] T. Dombre, U. Frisch, J. M. Greene, M. Hénon, A. Mehr, and A. M. Soward, *J. Fluid Mech.* **167**, 353 (1986).
- [31] M. Feingold, L. P. Kadanoff, and O. Piro, *J. Stat. Phys.* **50**, 529 (1988).
- [32] A. H. Boozer, Plasma Confinement in *Encyclopedia of Physical Science and Technology*, Volume 13, Page 1 (Academic Press, New York, 1992).
- [33] V. I. Arnold, *Mathematical Methods of Classical Mechanics* (Springer-Verlag, New York, 1989).
- [34] A. H. Boozer, *Phys. Fluids* **26**, 1288 (1983).
- [35] J. Pöschel, *Communications on Pure and Applied Mathematics*, Vol. XXXV, 653 (1982).
- [36] D. Ruelle, *Phys. Math. IHES* **50**, 275.
- [37] D. Ruelle, *Elements of Differentiable Dynamics and Bifurcation Theory* (Academic Press, San Diego, 1989).
- [38] Leonhard Euler, *Novi Comentarior Acad. Sci. Petropolitanae* **14**, 270 (1769).
- [39] A.J. Lichtenberg and M.A. Lieberman, *Regular and Stochastic Motion* (Spring-Verlag, New York, 1983).
- [40] G. M. Zaslavsky, R. Z. Sagdeev, D. A. Usikov and A. A. Chernikov, *Weak Chaos and Quasi-Regular Patterns* (Cambridge University Press, 1991).

## Figures

FIG. 1: The finite time Lyapunov exponent  $\lambda$  is related to the largest eigenvalue of the metric tensor  $\Lambda$  by  $\ln \Lambda = 2\lambda t$  (uptriangles).  $\theta$  and  $\phi$  are the polar and azimuthal angles of the  $\hat{\mathbf{s}}$  vector,  $\ln(d\theta/dt)$  (downtriangles) and  $\ln(d\phi/dt)$  (circles). (a) Standard map with  $k = 1.5$ , at point  $(0.3, 0.6)$ ; (b) Extended standard map with  $k = 1.5$  and  $\Delta = \sqrt{3}$ , at point  $(0.3, 0.6, 0.8)$ .

FIG. 2: The distribution of finite time Lyapunov exponents along a single trajectory peaks around the infinite time Lyapunov exponent. The finite time Lyapunov exponents,  $\lambda(\xi, t)$ , are evaluated at fixed  $t$ . Extended standard map with  $k = 3.0$  and  $\Delta = \sqrt{3}$ ,  $t = 20$  iterations.

FIG. 3: The residue, or difference, between the distribution of finite time Lyapunov exponents and a Gaussian distribution, decreases as  $t$  increases. Circles are for extended standard map with  $k = 10.0$  and  $\Delta^2 = 3$ . Triangles are for standard map with  $k = 10.0$ . Dashed and Solid lines are given by  $Residue = 0.347/\sqrt{t} + 0.018$  and  $Residue = 0.31/\sqrt{t} + 0.0026$ .

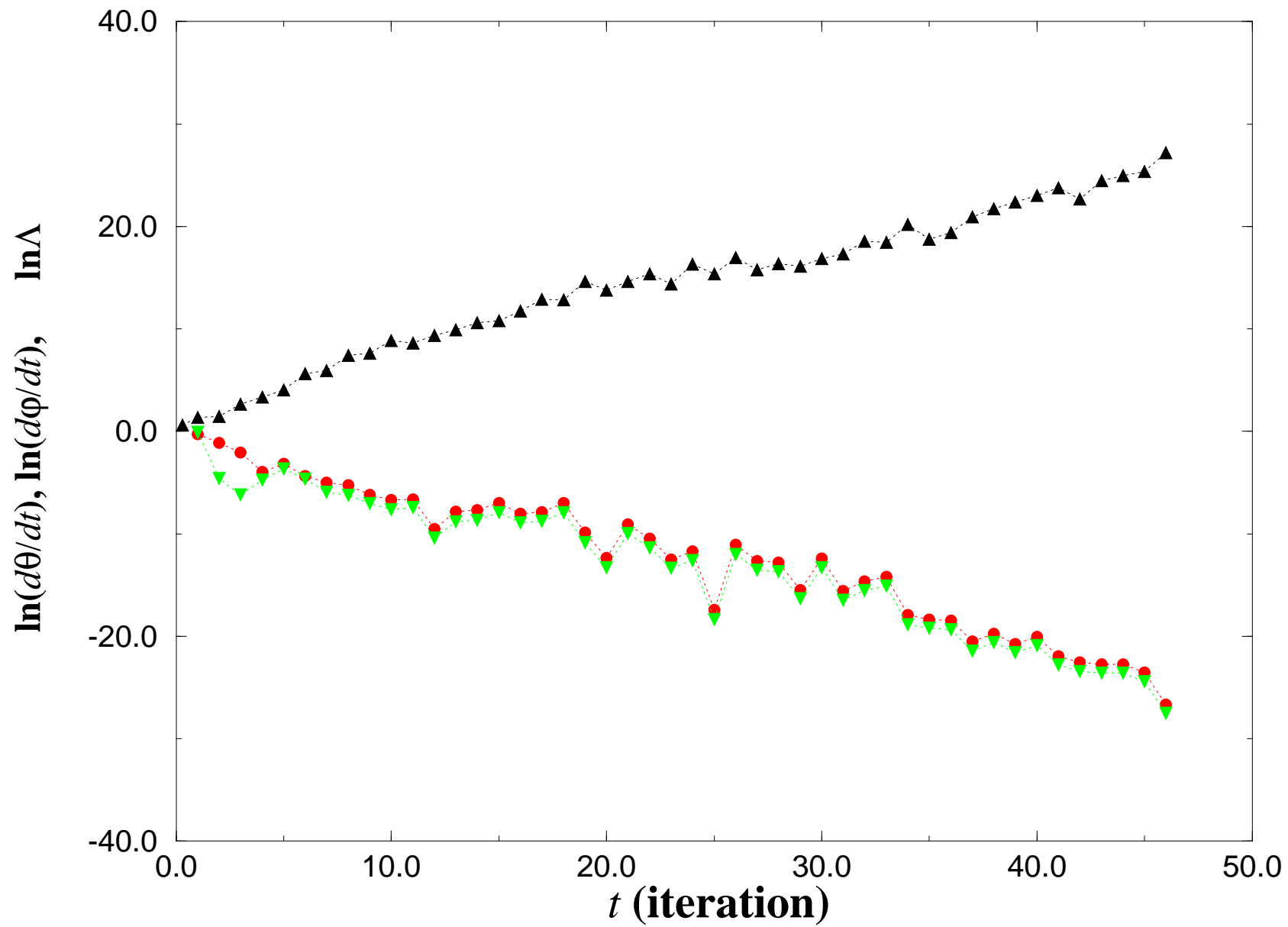
FIG. 4: The standard deviation of the distribution of finite time Lyapunov exponents decreases the further the flow is from being integrable (larger  $k$ ). Uptriangles and circles are for extended standard map with  $t = 40$  and 20 iterations, respectively. Downtriangles are for standard map with  $t = 40$  iterations.

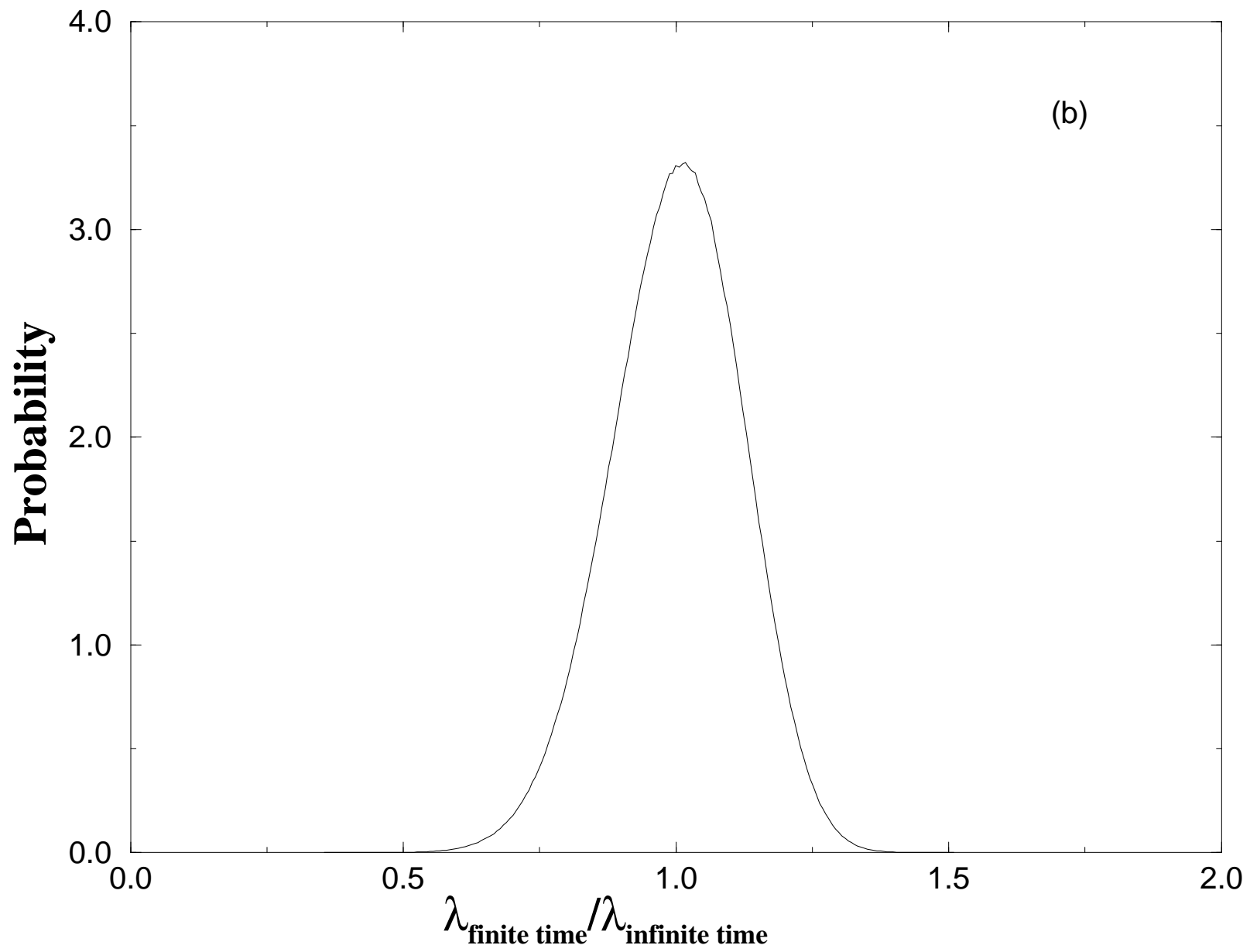
FIG. 5: The standard deviation of the distribution of finite time Lyapunov exponents scales as  $1/\sqrt{t}$ . Uptriangles are for standard map with  $k = 10.0$ . Circles are for extended standard map with  $k = 10.0$  and  $\Delta = \sqrt{3}$ . Dashed and Solid lines are given by  $\sigma = 0.785/\sqrt{t}$  and  $\sigma = 0.382/\sqrt{t}$ .

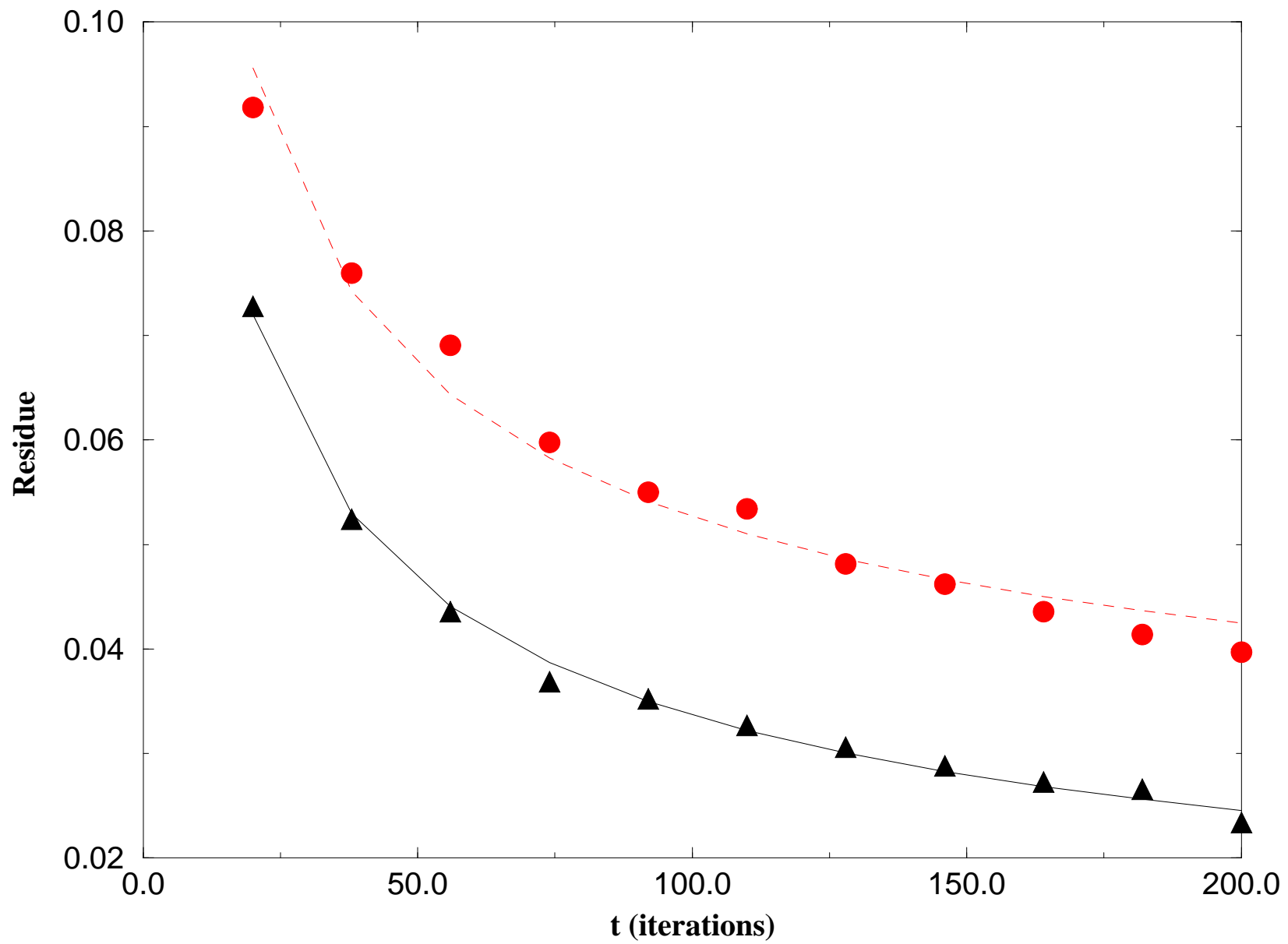
FIG. 6:  $\Delta(\xi, t) \equiv |\hat{\mathbf{s}} \cdot \nabla_0(\lambda t) + \nabla_0 \cdot \hat{\mathbf{s}}|$  exponentially converges to zero. Uptriangle:  $\Delta(\xi, t)$  is evaluated at point  $(0.3, 0.6, 0.8)$  for extended standard map with  $k = 1.5$ . Circles:  $\Delta(\xi, t)$  is evaluated at point  $(0.1, 0.2, 0.75)$  for ABC map with  $A = B = C = 1$ .

FIG. 7: Extended standard map with  $k = 2.0$  and  $\Delta = \sqrt{3}$ . (a) The Lyapunov exponents,  $\lambda(t = 30)$ , were sampled with equal spacing along an  $\hat{\mathbf{e}}$  line, an  $\hat{\mathbf{m}}$  line and an  $\hat{\mathbf{s}}$  line (all starting at  $(0.1, 0.1, 0.8)$ ). These values are plotted against the distance along the lines; (b) The correlation function for the Lyapunov exponents in the  $\hat{\mathbf{s}}$  direction (solid), in the  $\hat{\mathbf{m}}$  direction (dashed) and in the  $\hat{\mathbf{e}}$  direction (dotted).

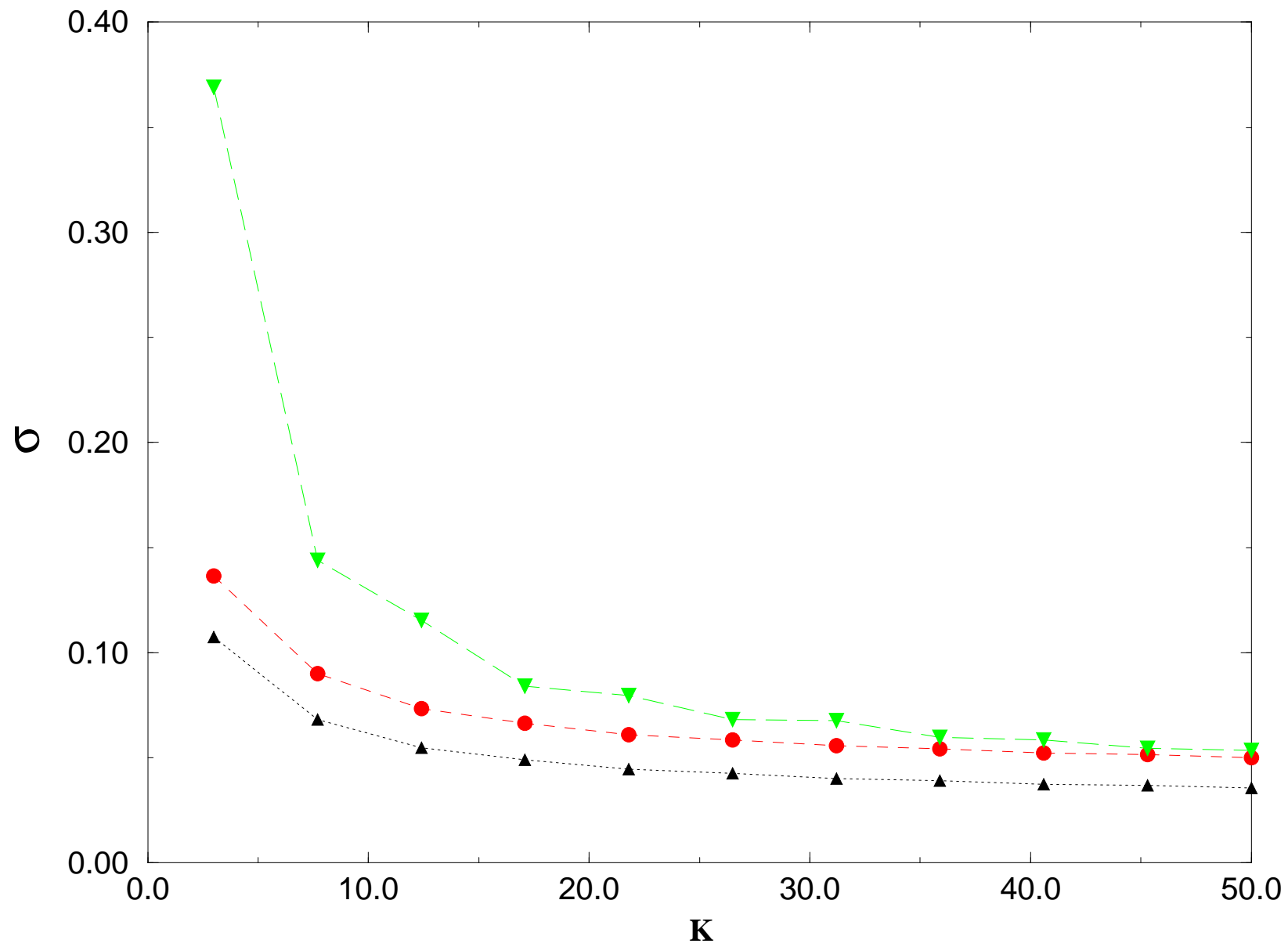
FIG. 8: The finite time Lyapunov exponent ( $\lambda$ ), the  $\hat{\mathbf{e}}$  and  $\hat{\mathbf{m}}$  components of the  $\hat{\mathbf{s}}$  line curvature ( $\kappa_e$  and  $\kappa_m$ ), are plotted as functions of distance along an  $\hat{\mathbf{s}}$  line. The calculation was done for ABC map with  $A = B = C = 1$ . Only the magnitudes of the curvature are used for the log-linear plots.

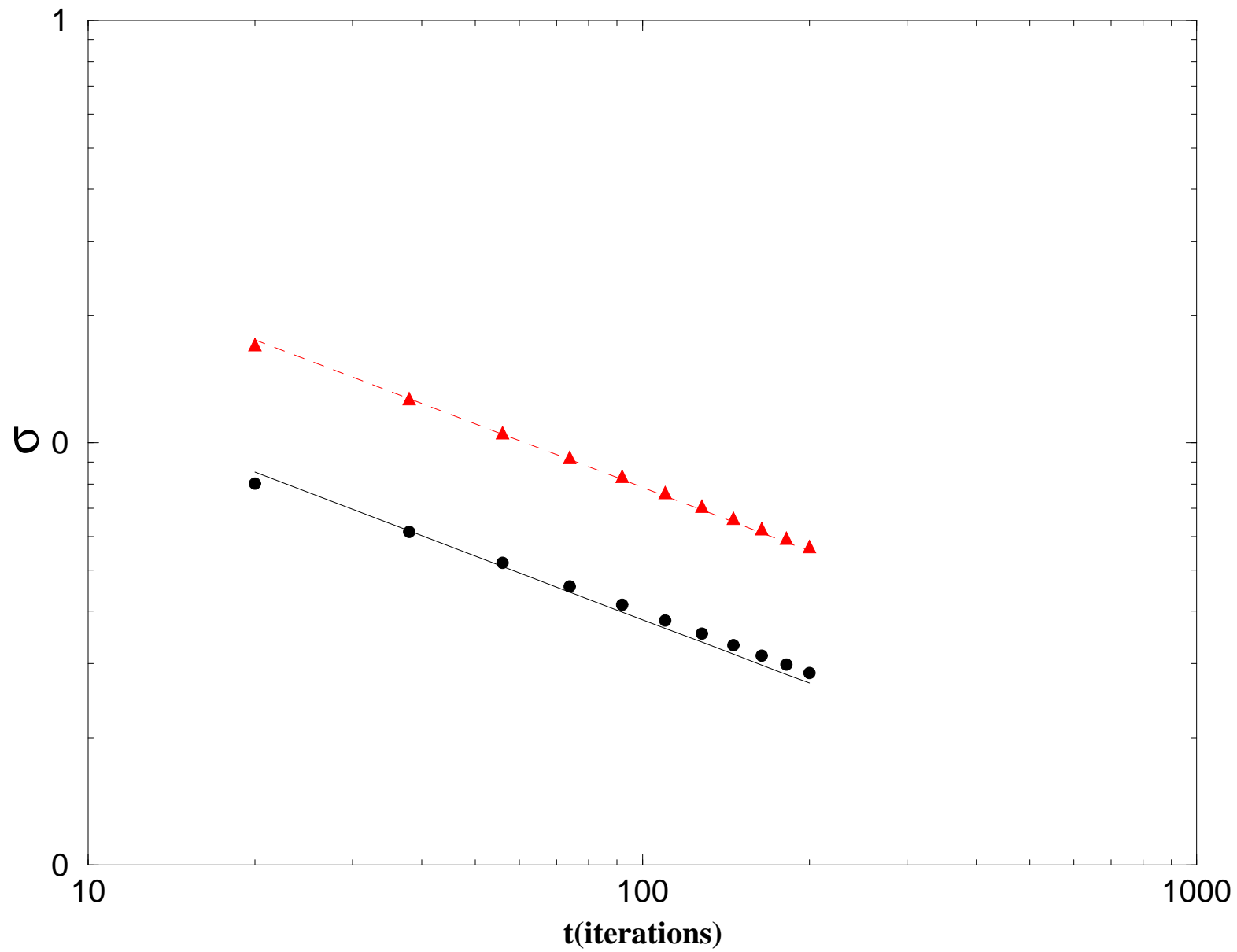


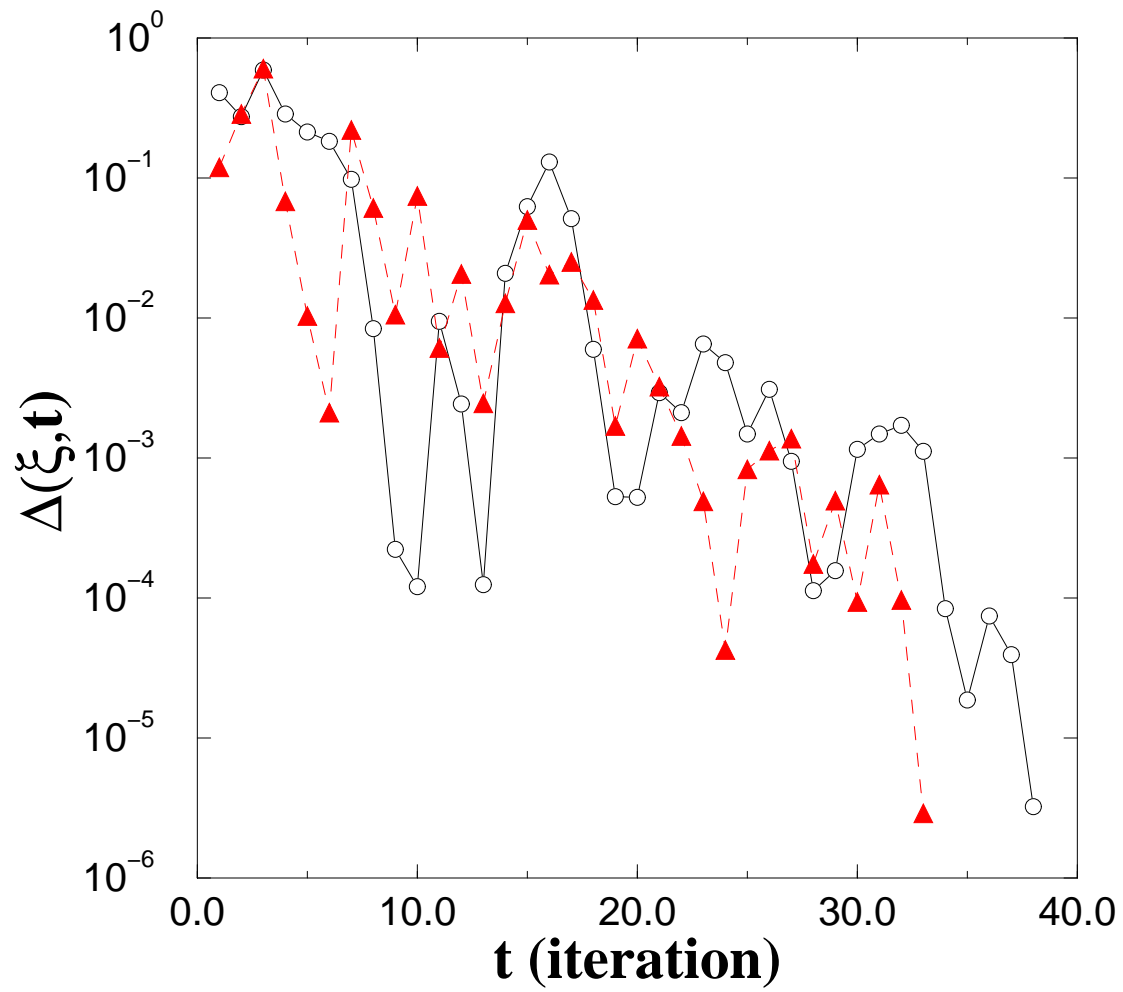




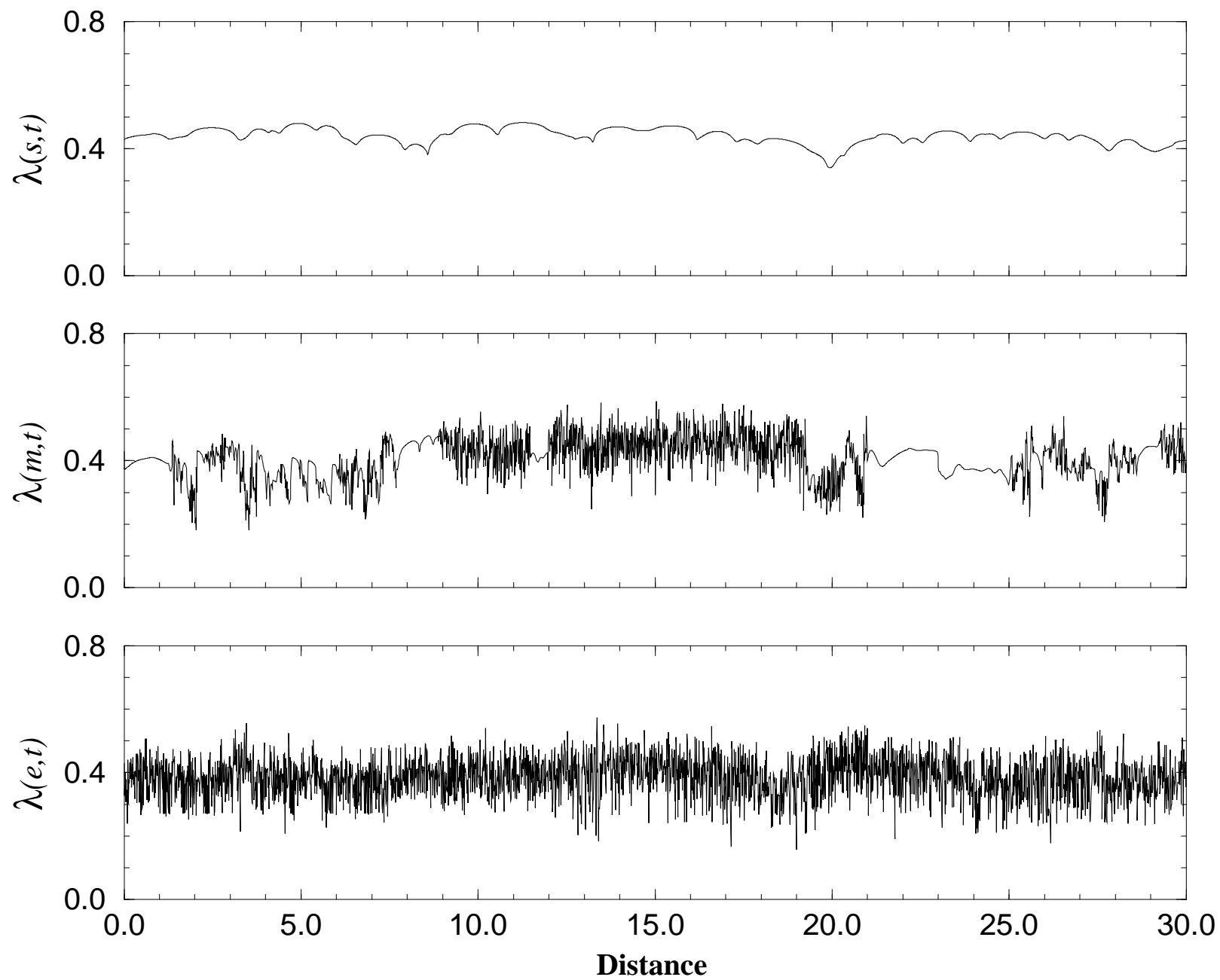








**(a)**



(b)

